Two new Thermocyclops species (Copepoda, Cyclopoida) from Thailand, with notes on the genus phylogeny inferred from 18S and ITS sequences

Article *in* Zoologischer Anzeiger - A Journal of Comparative Zoology · July 2017

DOI: 10.1016/j.jcz.2017.07.003

CITATIONS
7

READS
458

3 authors, including:

Tomislav Karanovic
University of Tasmania
95 PUBLICATIONS **1,278** CITATIONS

SEE PROFILE

La-orsri Sanoamuang
Khon Kaen University, Thailand
133 PUBLICATIONS **1,422** CITATIONS

SEE PROFILE

Zoologischer Anzeiger 269 (2017) 26–47

Contents lists available at ScienceDirect

Zoologischer Anzeiger

journal homepage: www.elsevier.com/locate/jcz

Zoologischer Anzeiger

Research paper

Two new *Thermocyclops* species (Copepoda, Cyclopoida) from Thailand, with notes on the genus phylogeny inferred from 18S and ITS sequences

Tomislav Karanovic[a,b,*], Kamonwan Koomput[c], La-orsri Sanoamuang[c,d]

[a] Sungkyunkwan University, College of Science, General Studies Building, Room 51311, Suwon 16419, Republic of Korea
[b] University of Tasmania, Institute for Marine and Antarctic Studies, Hobart, Tasmania 7001, Australia
[c] Khon Kaen University, Applied Taxonomic Research Centre, Department of Biology, Khon Kaen 40002, Thailand
[d] Khon Kaen University, International College, Khon Kaen 40002, Thailand

ARTICLE INFO

Article history:
Received 30 January 2017
Received in revised form 29 April 2017
Accepted 17 July 2017
Available online 23 July 2017

Keywords:
Cave
Mesocyclops affinis
Thermocyclops parahastatus sp. nov
Thermocyclops thailandensis sp. nov
Taxonomy

ABSTRACT

With nearly 80 valid species, the genus *Thermocyclops* Kiefer, 1927 is one of the most speciose members of the family Cyclopidae. Although its centre of diversity is in the Sub-Saharan Africa, different species can be found in almost any non-glaciated part of the world. Six of them have been recorded so far from Thailand, all from lacustrine environments and with very wide distribution. It was therefore surprising to discover two endemic new species living sympatrically in a single cave. We describe their morphology in detail and assess affinities between them, and among them and the rest of their congeners. Judging by their morphology, one species has no close living relatives, while the other is very similar to the African *T. hastatus* Kiefer, 1952 and the Carribean *T. antillensis* Herbst, 1986. We use 18S and ITS nuclear markers to assess phylogenetic relationships of the new species, as well as to test the monophyly of *Thermocyclops* and a closely related genus *Mesocyclops* Sars, 1914. Both morphological data and reconstructed phylogenies reveal the two new species as only distantly related, which probably facilitates their sympatry. We were unable to challenge monophyly of either *Mesocyclops* or *Thermocyclops*, despite their diagnosis being essentially based on a single morphological character.

1. Introduction

During a survey of subterranean habitats in northern Thailand we discovered an interesting copepod fauna in Tham Chom Sin cave (Fig. 1), which consisted of two new species from the cyclopoid genus *Thermocyclops* Kiefer, 1927, a widely distributed South East Asian cyclopoid *Mesocyclops affinis* Van de Velde, 1987, and one new species from the harpacticoid genus *Parapseudoleptomesochra* Lang, 1965. The aim of this paper is to provide taxonomic descriptions of the new *Thermocyclops* species, and to assess their affinities based both on morphological and molecular characters. We choose two nuclear markers, 18S ribosomal RNA (18S thereafter) and the internal transcribed spacer (ITS), mostly based on the availability of comparative data for this and other closely related genera. In addition to sequencing the new species of *Thermocyclops*, we also sequence *M. affinis*, as no molecular data are available for this species so far.

Emerging trends in systematic biology focus on examining more than one line of evidence for species delimitation (Marshall et al., 2006; Pons et al., 2006; Wiens, 2007; Carstens et al., 2013), and there is no question that a combined morphological and molecular approach results in a much more thorough study (Will et al., 2005; Padial et al., 2010). In recent years several studies on copepods showed that molecular data can help answer questions related to cryptic speciation (Bláha et al., 2010; Hamrova et al., 2012; Karanovic et al., 2016), invasions of new habitats and colonization pathways (Lee et al., 2003; Winkler et al., 2008; Karanovic and Cooper, 2011a, 2012), anthropogenic translocation (Karanovic and Krajicek, 2012a), short-range endemism (Karanovic and Cooper, 2011a), suitability of novel micro-morphological characters (Karanovic and Kim, 2014b), population structure and interbreeding (Burton and Lee, 1994; Ganz and Burton, 1995; Palmer and Edmands, 2000; Ellison and Burton, 2008; Hwang et al., 2012), phylogeography (Edmands, 2001; Denis et al., 2009; Ki et al., 2009; Handschumacher et al., 2010; Peterson et al., 2013), and definition

* Corresponding author at: University of Tasmania, Institute for Marine and Antarctic Studies, Hobart, Tasmania 7001, Australia.
E-mail address: Tomislav.Karanovic@gmail.com (T. Karanovic).

http://dx.doi.org/10.1016/j.jcz.2017.07.003
0044-5231/

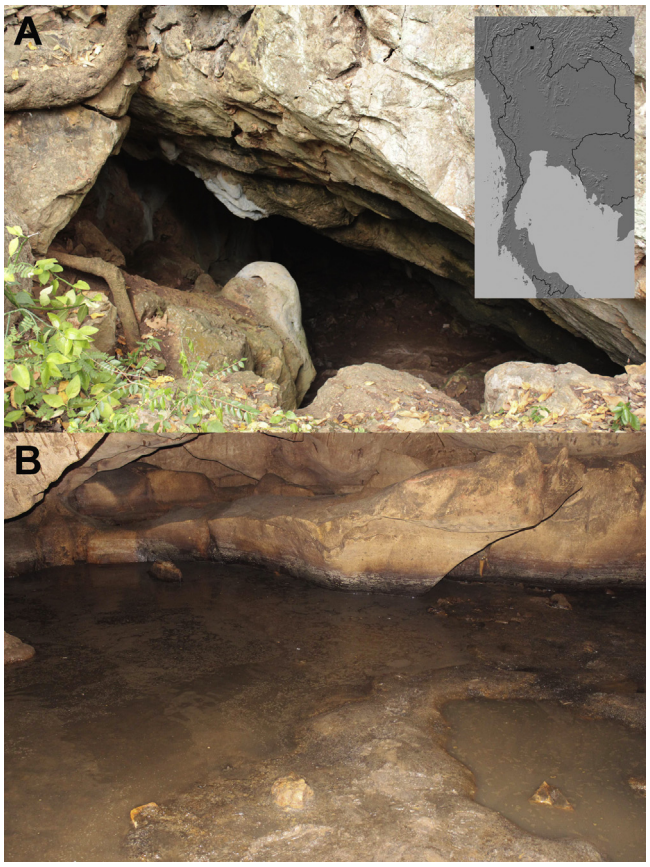

Fig. 1. Tham Chom Sin cave, the type locality for both new *Thermocyclops* Kiefer, 1927 species: (A) cave entrance, (B) pool of percolating water where species were collected. Inset shows the location of Tham Chom Sin cave in northern Thailand.

of supraspecific taxa in conservative genera or families (Huys et al., 2006, 2012; Karanovic and Cooper, 2011b; Karanovic and Krajicek, 2012b). However, the number of sequenced taxa and markers is still very low for this crustacean group. A quick search of the National Center for Biotechnology Information (NCBI) database (https://www.ncbi.nlm.nih.gov; accessed on 10 January 2017) shows that copepods have 860,507 nucleotides (DNA and RNA sequences) and only 202 short genetic variations (SNPs) available, which is in orders of magnitude less than some well-studied animal groups of comparable size, such as birds (6,859,595 and 24,415,900 respectively) and mammals (43,547,553 and 643,238,580 respectively), as well as some groups of large crustaceans, such as decapods (1,379,865 and 1380 respectively) and isopods (2,844,248 and 0 respectively). This is still better than in some other crustacean groups of comparable size, such as amphipods (207,022 and 0 respectively) and ostracods (69,038 and 0 respectively). Clearly, more sequencing effort is needed for crustaceans, for which all together we only have 6,158,541 nucleotides and 1721 SNPs, compared, for example, with 18,484,096 nucleotides and 11,469,942 SNPs we have for insects.

Members of both *Thermocyclops* and *Mesocyclops* Sars, 1914 are common in lacustrine planktonic faunas in tropical and temperate latitudes worldwide (Reid, 2003). Their members are usually large species that are numerous, omnivorous, and capable of surviving in challenging environmental conditions (Williamson, 1986). They are among the most speciose cyclopoid genera, and their greatest diversity is in the tropics (Dussart and Defaye, 2006). In subterranean waters they are rather rare, and usually present either in arid areas where surface water is scarce (Dumont and Maas, 1985; Fiers et al., 1996; Karanovic, 2006) or living as stygophiles, most commonly in wells (Ito, 1970; Pesce and Maggi, 1981; Herbst, 1986). Several widely distributed species have been found occasionally in caves (Dussart and Defaye, 2006), but usually in very low numbers compared to their surface populations (as stygoxenes). No species has been found yet with troglomorphic adaptations (stygobiont), which indicates that these cyclopoids are only starting to colonize subterranean environments. The most recent key to species was provided by Hołyńska et al. (2003) for *Mesocyclops* and by Mirabdullayev et al. (2003) for *Thermocyclops*. The phylogeny of *Mesocyclops* was assessed both based on morphological (Hołyńska, 2006) and molecular characters (Wyngaard et al., 2010), while we are still awaiting for anything similar for *Thermocyclops*. Since Kiefer (1927) separated *Termocyclops* from *Mesocyclops* (first as a subgenus) many authors noted that the single generic distinguishing character is the insertion of spine on the fifth leg (Lindberg 1942; Rylov 1948; Einsle 1970; Ueda and Reid, 2003; Hołyńska, 2006). Also, some taxa were described with transitional morphological characters, such as the South American *M. bernardi* Petkovski, 1954; this species was later transferred into the genus *Diacyclops* Kiefer, 1927 by Reid (1993), although not without controversy (Karanovic, 2000). However, the monophylies of either *Mescocyclops* or *Thermocyclops* have never been explicitly challenged. We aimed to test this by using our molecular markers and including a few more genera in our analyses.

The cyclopoid fauna of Thailand today counts 43 species (Sanoamuang, 1999), with seven species from the genus *Mesocyclops* (including *M. affinis*) and six species from the genus *Thermocyclops*. No endemic elements from either genus have been reported so far, and most members are widely distributed tropical species. For example, *M. affinis* was originally described from Papua New Guinea (Van de Velde, 1987), but was later found also in Indonesia, Malaysia, and Thailand (Dussart and Fernando, 1988; Hołyńska, 1994; Hołyńska et al., 2003; Alekseev and Sanoamuang, 2006), and *T. crassus* (Fisher, 1853) is almost cosmopolitan (Rylov, 1948; Dussart, 1969; Monchenko, 1974; Kiefer, 1978; Duchovnay et al., 1992; Gutiérrez-Aguirre and Suárez-Morales, 2000; Hołyńska et al., 2003; Dussart and Defaye, 2006; Chaicharoen et al., 2011). Therefore, it was a big surprise to discover two endemic new species of *Thermocyclops* in a single cave in orthern Thailand. It was not, however, surprising to find them together with a member of the genus *Mesocyclops*, as various species from these two genera form zooplankton communities in many parts of the world (Ruttner, 1952; Gophen, 1986; Maier, 1996).

2. Material and methods

Samples were taken with a hand net (mesh size 30 μm), preserved in the field in 95% ethanol, sorted and preliminarily identified in the laboratory in glycerol, and kept in a refrigerator in 99.9% ethanol. All four copepod species were found by the second author in the same pool in Tham Chom Sin cave (Fig. 1) on each of the three sampling events: 7 December 2014, 5 April 2015, and 10 June 2016. The cave is situated at the foot of a local hill, about 75 m long (Vogt, 2013), mostly horizontal, and the pool is about 2 m in diameter, filled with percolating water, and situated at the very end of the cave. Water conditions were measured only on the last sampling date: temperature 26.6 °C, pH 7.3, conductivity 639.3 μS/cm, dissolved oxygen 4.7 mg/L, nitrate 1.1 mg/L, and phosphate 0.56 mg/L. All specimens used for our molecular analyses were sacrificed(*M. affinis*: seven females; *T. parahastatus*: six females; *T. thailandensis*: seven females), but specimens used for morphological analyses are preserved either in alcohol, on permanent glass slides, or on scanning electron microscope (SEM) stubs, and deposited in the Western Australian Museum (WAM), Perth, Australia. The number of examined specimens is given for each new *Thermocyclops* species separately below. Additionally, we deposited the following

specimens of *Mesocyclops affinis*: one ovigerous female dissected on one slide (WAM C55904); one male and eight females (three ovigerous) together in one alcohol vial (WAM C55905), collected on 7 December 2014. Specimens that were dissected were mounted on microscope slides in Faure's medium (Stock and von Vaupel Klein, 1996). For the urosome or the entire animal, two human hairs were mounted between the slide and coverslip. All line drawings were prepared using a drawing tube attached to a Leica MB2500 phase-interference compound microscope. Specimens that were not drawn were examined in glycerol in toto and, after examination, were stored in 99.9% ethanol. Specimens for SEM were dehydrated in progressive ethanol concentrations, transferred into pure isoamylacetate, critical-point dried, mounted on stubs, coated in gold, and observed under a Hitachi S-4700 microscope on the in-lens detector, with an accelerating voltage of 10 kV and working distances between 12.3 and 13.4 mm. The terminology for macromorphological characters follows Huys and Boxshall (1991), except for the numbering of setae on the caudal rami and small differences in the spelling of some appendages (antennula, mandibula, maxillula instead of antennule, mandible, maxillule), as an attempt to standardise the terminology for homologous appendages in different crustacean groups. Cuticular organs (sensilla and pores) were examined on some somites; we made no attempt to make a detailed survey. The most prominent morphological differences between the two new species were indicated with arrowheads on selected illustrations of the second presented species.

Specimens for molecular analyses were examined without dissecting under a Leica MB2500 phase-interference compound microscope (objective 63x dry) in glycerol. After examination they were returned to 99.9% ethanol. In the first step of the DNA extraction specimens were kept for 2–3 h in distilled water. LaboPass Tissue Mini extraction kit (Cosmo Genetech Co., LTD, Korea) was used in all further steps of extraction. Fragments of 18S rRNA gene were amplified with primers 18s329 and 18sI from Spears et al. (1992), with the same PCR settings as described in Karanovic and Krajicek (2012a). ITS region was amplified with primers forward ITS 3 (White et al., 1990) and reverse ITS 10 (Goetze, 2003), with the following PCR settings: initial denaturation for 50 s at 95 °C, 35 cycles of denaturation for 30 s at 95 °C, annealing for 30 s at 55 °C, extension for 1 min at 72 °C, and final extension for 7 min at 72 °C. PCR products from this reaction were used as a template for the next PCR reaction, which was carried out with the primer pair ITS 3 and ITS 4 from White et al. (1990), under the same PCR settings. For all amplifications PCR reactions were carried out in 25 μL volumes, containing: 5 μL of DNA template (or 2.5 μL in the case of second PCR reaction for ITS), 2.5 μL of 10 x ExTaq Buffer, 0.25 μL of TaKaRa Ex Taq (5 units/μL), 2 μL of dNDTP Mixture (2.5 mM each), 1 μL each primer, and 13.25 μL (or 15.75 μL in the case of the second PCR reaction for ITS) of distilled water. The PCR products were electrophoresed on 1% agarose gels, and, if DNA was present, the products were purified for sequencing reactions using the LaboPass PCR Purification Kit. DNA was sequenced on an ABI automatic capillary sequencer (Macrogene, Seoul, South Korea) using the same set of primers. A total of 11 specimens were successfully sequenced for ITS and three specimens for 18S (Table 1); fragments ranged in length from 244 to 372 bases for ITS, while those for 18S were all trimmed to 328 bases. Another 70 sequences (32 of 18S and 47 of ITS), identified to belong to genera *Thermocyclops, Mesocyclops, Diacyclops, Cyclops* Müller, 1785, or *Macrocyclops* Claus, 1893, were downloaded from GenBank and included in our analyses. *Cyclops* was used for rooting our ITS trees and *Macrocyclops* for rooting our 18 trees.

Obtained sequences were visualized using Finch TV version 1.4.0 (http://www.geospiza.com/Products/finchtv.shtml), checked for the quality of signal and sites with possible low resolution, and corrected by comparing forward and reverse strands. BLAST (Altschul et al., 1990) analyses of the GenBank database were used to check that the obtained sequences were copepod in origin and not contaminants. Sequences were aligned in MEGA with ClustalW (Thompson et al., 1994) using default parameters. The alignment was again manually checked and corrected where necessary; all sequences of 18S were trimmed after alignment to 329 overlapping sites, while those of ITS were analysed using their original lengths (ranging from 224 to 395 bases). Distances between sequences in the alignment were calculated using Kimura 2-paramter (K2P) model (Kimura, 1980) with uniform rates and pairwise deletion. The following phylogenetic analyses were performed: Maximum Likelihood (ML) using MEGA 7 (Kumar et al., 2016), and Bayesian Inference (BI) using MrBayes v3.2.6 (Huelsenbeck and Ronquist, 2001; Ronquist and Huelsenbeck, 2003; Ronquist et al., 2012). For the best fit, evolutionary model program jModelTest 2.1.6 (Darriba et al., 2012; Guindon and Gascuel, 2003) was used with the Akaike information criterion (Hurvich and Tsai, 1989). The ML method used fast stepwise-addition as the search method, with all gaps treated as missing data; the bootstrap values (Felsenstein, 1985) were calculated with 1000 pseudo-replicates. The BI analysis used fixed priors for both base and state frequencies (calculated for the best fit model) with four chains run simultaneously for 2 million generations in two independent runs, sampling trees every 200 generations. Of the four chains three were heated and one was cold; the temperature value ("Temp" command in MrBayes) was 0.1 (default option). Trees from each MrBayes run were combined and a burn-in of 5000 trees (25% of the total) was chosen, with a > 50% posterior probability consensus tree constructed from the remaining trees.

3. Results

3.1. Molecular analyses

The GTR + I + G (Rodríguez et al., 1990) was found to be the best fit evolutionary model for both datasets based on the Akaike information criterion. The 18S alignment contained only one gap, introduced with sequences of *Mesocyclops dissimilis* Defaye and Kawabata, 1993 (GenBank accession code KR048719) and *Diacyclops uruguayensis* (Kiefer, 1935)(GenBank accession code HQ008753); all other sequences being of 328 base pairs. Several sequences from GenBank identical to those used in our 18S dataset were excluded, and two sequences were excluded because they could not be unambiguously aligned with the rest: *Mesocyclops thermocyclopoides* Harada, 1931 (GenBank accession code EF581894) and *Mesocyclops* sp. (GenBank accession code KM023644); we suspect that they represent either contamination or misidentification. The ITS dataset was analysed with original (submitted) lengths and it contained several gaps. Also, identical sequences were excluded, and five GenBank sequences were excluded because they could not be unambiguously aligned with the rest: *Thermocyclops minutus* Lowndes, 1934 (GenBank accession code EF114369), *Thermocyclops inversus* (Kiefer, 1936) (GenBank accession code EF114368), *Thermocyclops* sp. (GenBank accession code HQ845965), *Mesocyclops* sp. (GenBank accession code KR013057), and *Mesocyclops* sp. (GenBank accession code KP995487). It is also possible that they represent either contamination or misidentification, but more caution is necessary in interpretation, as ITS is a non-functional and very variable region. After 2 million generations runs in MrBayes, the final standard deviation of split frequencies had reduced to 0.006 and the potential scale reduction factor (PSRF) was ~1.0 for all parameters, suggesting that convergence had been reached. Rates of chain mixing were between 20% and 40%.

Table 1
List of specimens sequenced and their GenBank accession codes.

GenBank	Species	Marker	Bases	Date	Sex
KY978846	*Thermocyclops parahastatus*	18S	328	10 June 2016	female
KY978847	*Thermocyclops thailandensis*	18S	328	10 June 2016	female
KY978848	*Thermocyclops thailandensis*	18S	328	10 June 2016	female
KY978835	*Thermocyclops thailandensis*	ITS	224	10 June 2016	female
KY978836	*Thermocyclops thailandensis*	ITS	372	5 April 2015	female
KY978837	*Thermocyclops thailandensis*	ITS	257	5 April 2015	female
KY978838	*Thermocyclops thailandensis*	ITS	289	5 April 2015	female
KY978839	*Thermocyclops parahastatus*	ITS	363	10 June 2016	female
KY978840	*Thermocyclops parahastatus*	ITS	241	10 June 2016	female
KY978841	*Mesocyclops affinis*	ITS	364	5 April 2015	female
KY978842	*Mesocyclops affinis*	ITS	286	5 April 2015	female
KY978843	*Mesocyclops affinis*	ITS	274	5 April 2015	female
KY978844	*Mesocyclops affinis*	ITS	245	5 April 2015	female
KY978845	*Mesocyclops affinis*	ITS	228	5 April 2015	female

Average intraspecific divergences for the three species from Thailand ranged from 0% to 0.9% for ITS (Supplementary Table 2) and were 0.3% for 18S in *Thermocyclops thailandensis*, our only multisequence species for this marker (Supplementary Table 3). Average divergence values between the two new species of *Thermocyclops* were 28.3% for ITS and 3.6% for 18S, while those between *T. parahastatus* and *Mesocyclops affinis* were 22.7% for ITS, and those between *T. thailandensis* and *M. affinis* were 32.4% for ITS (we had no 18S sequences for *M. affinis*). The interspecific divergences in 18S between the two new *Thermocyclops* species are comparable to those among Australian and European members of the genus *Diacyclops* (excluding the South American *D. uruguayensis*, see below), which ranged from 0.3% to 3.8% and averaged at 1.67% (Supplementary Table 3). The interspecific divergences in ITS among the three species from Thailand were in an order of magnitude higher than those between the three members of the genus *Cyclops*, which did not exceed 2.34% (Supplementary Table 2), suggesting that the new *Thermocyclops* species are only distantly related.

Our 18S phylogenetic tree (Fig. 2) could not challenge monophyly of neither *Mesocyclops* nor *Thermocyclops*. However, both clades were supported with moderate posterior probabilities in the BI analysis (93% and 85% respectively) but with week bootstrap values in the ML analysis (41% and 45% respectively). In addition, there were four problematic taxa on the tree. Two were already mentioned above, as causing a gap in our alignment: *D. uruguayensis* and *M. dissimilis*. Two others are *Mesocyclops darwini* Dussart and Fernando, 1988, which was nested deeply within the *Thermocyclops* clade, and an unidentified species of *Thermocyclops*, nested deeply within the *Diacyclops* clade. The *Diacyclops* clade was supported by maximum posterior probability in the BI analysis, so *Thermocyclops* sp. could be a misidentification. The *Macrocyclops* clade was only moderately supported. Several other clades were well supported on the 18S tree, including that suggesting a monophyly of *Termocyclops* and *Mesocyclops* (99% in BI, but only 69% in ML), as well as that suggesting *D. uruguayensis* as its sister clade (99% in BI and 88% in ML). Some sister-species relationships were relatively well supported (such as that between *Diacyclops crassicaudis* (Sars, 1863) and *D. bisetosus* (Rehberg, 1880)), as well as several basal clades in the genus *Mesocyclops*. However, many terminal branches were unresolved, forming extensive combs, which might be a consequence of a relatively small fragment of 18S analysed and the fact that 18S is a slow-evolving gene. The two new species were suggested as only remotely related. *Thermocyclops thailandensis* clustered together with an unidentified species or *Thermocyclops* (GenBank code HQ845972), and their average divergence was 0.75% (Supplementary Table 3). *Thermocyclops parahastatus* did nor cluster with any other congener, but was unresolved on the branch consisting of the abovementioned pair and *M. darwini* in the BI analysis, and this branch was not even recovered in the ML analysis. The average divergence value between *T. parahastatus* and any other species was never below 2.8% (all members of the genus *Thermocyclops* though; see Supplementary Table 3).

Surprisingly, our ITS phylogenetic tree (Fig. 3) also could not challenge monophyly of *Mesocyclops*; this clade receiving a maximum posterior probability in the BI analysis. It did, however, suggest that *Thermocyclops* could be paraphyletic, but caution is necessary in this interpretation of a highly variable, non-functional region. ITS also suggested that the two new species are only remotely related to each other, and without any close relative among sampled taxa. Divergence values between *T. parahastatus* and other species did not go below 10.6%, while those between *T. thailandensis* and other species did not go below 12.9% (Supplementary Table 2). The phylogenetic tree (Fig. 3) suggested *T. parahastatus* to be a sister clade to all other *Thermocyclops* and *Mesocyclops*, but this was supported only in the BI analysis (with maximum posterior probability) and not in the ML analysis. *Thermocyclops thailandensis* was a sister clade to all *Mesocyclops* in the BI analysis, but this clade received a low posterior probability (66%) and was also not recovered in the ML analysis. *Mesocyclops affinis* clustered together with several unidentified specimens of *Mesocyclops*, which might suggest their identity, although caution is necessary as there are two subclades in this clade (but not with very high support). Unfortunately, many GenBank sequences were identified only to the genus level, which impedes interpretation of phylogenetic relationships.

3.2. Taxonomy

3.2.1. *Thermocyclops parahastatus sp. nov.* (Figs. 4–7 & Suppl. Figs. 1–4)

3.2.1.1. Type locality. Northern Thailand, Phayao Province, Ban Tham village, Tham Chom Sin cave, pool on muddy floor filled with percolating water; coordinates of the cave entrance 19°04′52.68″N 100°04′24.74″E, 443 m above sea level.

3.2.1.2. Type material. Holotype: ovigerous female dissected on one slide (WAM C55906), collected from the type locality on 10 June 2016. Paratypes: two males and three males dissected on one slide each (WAM C55907–C55911), collected from the type locality on 10 June 2016; three males and five males together on one SEM stub (WAM C55912), collected from the type locality on 10 June 2016; one male, 14 females, and two copepodids together in one alcohol vial (WAM C55913), collected from the type locality on 5 April 2015; 11 males together in one alcohol vial (WAM C55914), collected from the type locality on 7 December 2014.

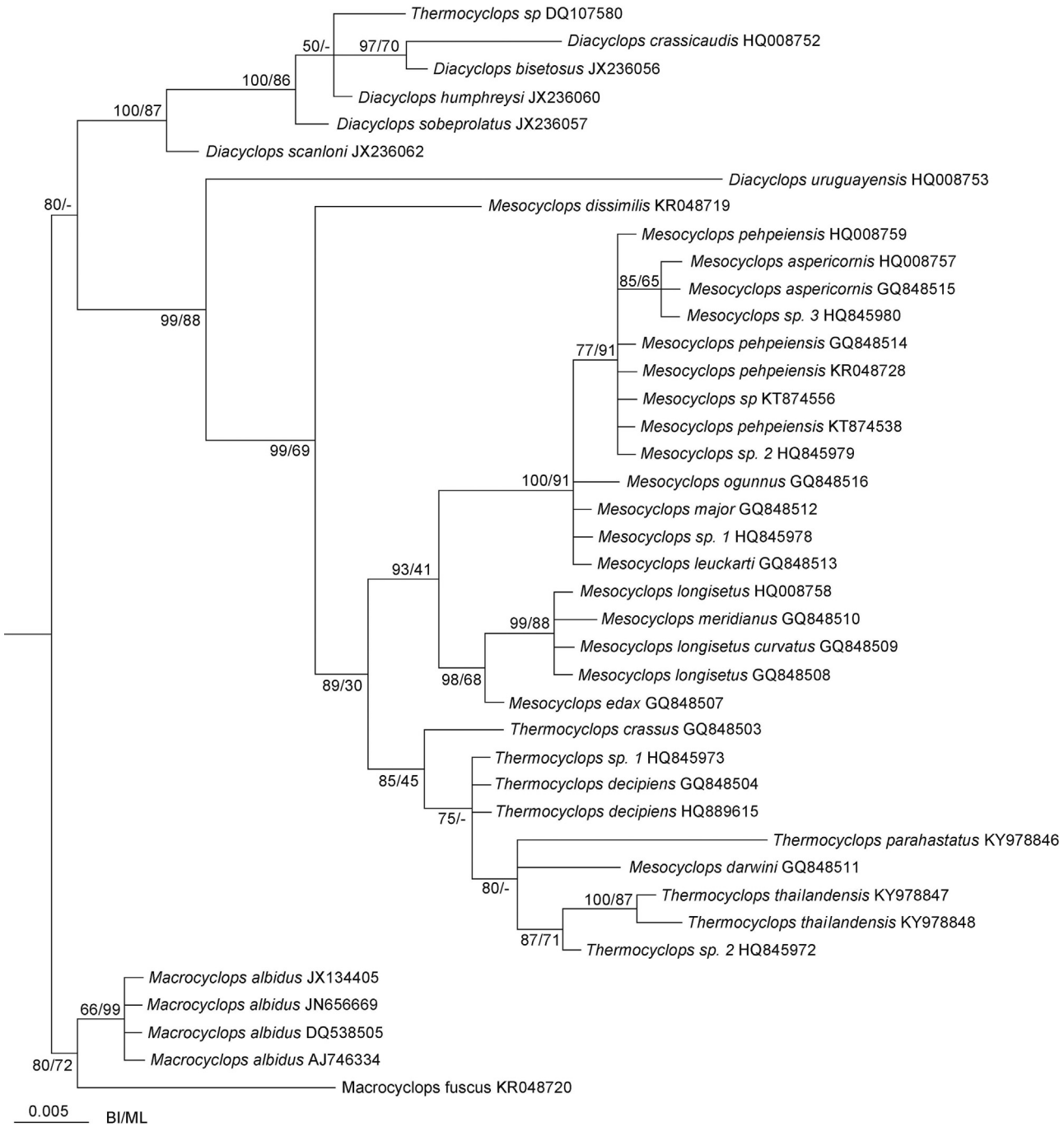

Fig. 2. Bayesian Inference (BI) tree based on 18S sequences of one specimen of *Thermocyclops parahastatus* sp. nov, two specimens of *T. thailandensis* sp. nov., and 32 other sequences from GenBank identified either as *Thermocyclps* Kiefer, 1927, *Mesocyclops* Sars, 1914, or *Diacyclops* Kiefer, 1927. The tree is computed using MrBayes, drawn to scale, and rooted with members of the genus *Macrocyclops* Claus, 1893. Numbers on the branches represent posterior probabilities in MrBuyes/bootstrap values from 1000 pseudo-replicates in MEGA 6 obtained from a maximum likelihood (ML) analysis (GTR + G + I model) of the same dataset. Codes after species names represent their GenBank accession numbers.

3.2.1.3. Etymology. The species name is a combination of the Greek adjective "para" (meaning "near") and the existing species name *hastatus*

3.2.1.4. Description of female. Based on holotype and eight paratypes. Body length, excluding caudal setae, from 705 to 780 μm. Habitus (Fig. 4A) robust in lateral view, with prosome/urosome ratio 2.1, and greatest width at posterior end of cephalothorax. Body length/width ratio about 2.6, cephalothorax 2.7 times as wide as genital double-somite. Free pedigerous somites without pronounced lateral expansions. Colour of preserved specimens yellowish and nauplius eye not visible. Integument (Figs. 4 and 5) on all somites generally smooth, without cuticular pits, with spinules only on anal somite and caudal rami, with irregular but mostly transverse short striae (especially frequent on genital double-somite; Figs. 5 D and 5 C), with cuticular pores on all somites, and sensilla on all but penultimate somite. Posterior hyaline fringes of cephalothorax and first two free prosomites smooth (Figs. 4 B and 5 B), those of third prosomite and first urosomite finely serrated (Figs. 4 C, D, 5 B, C), those of other urosomites (except anal somite) coarsely serrated (Figs. 4 D, F, 5 C, D, F). Rostrum (Suppl. Fig. 1A) well-developed, membranous, very broad, and furnished

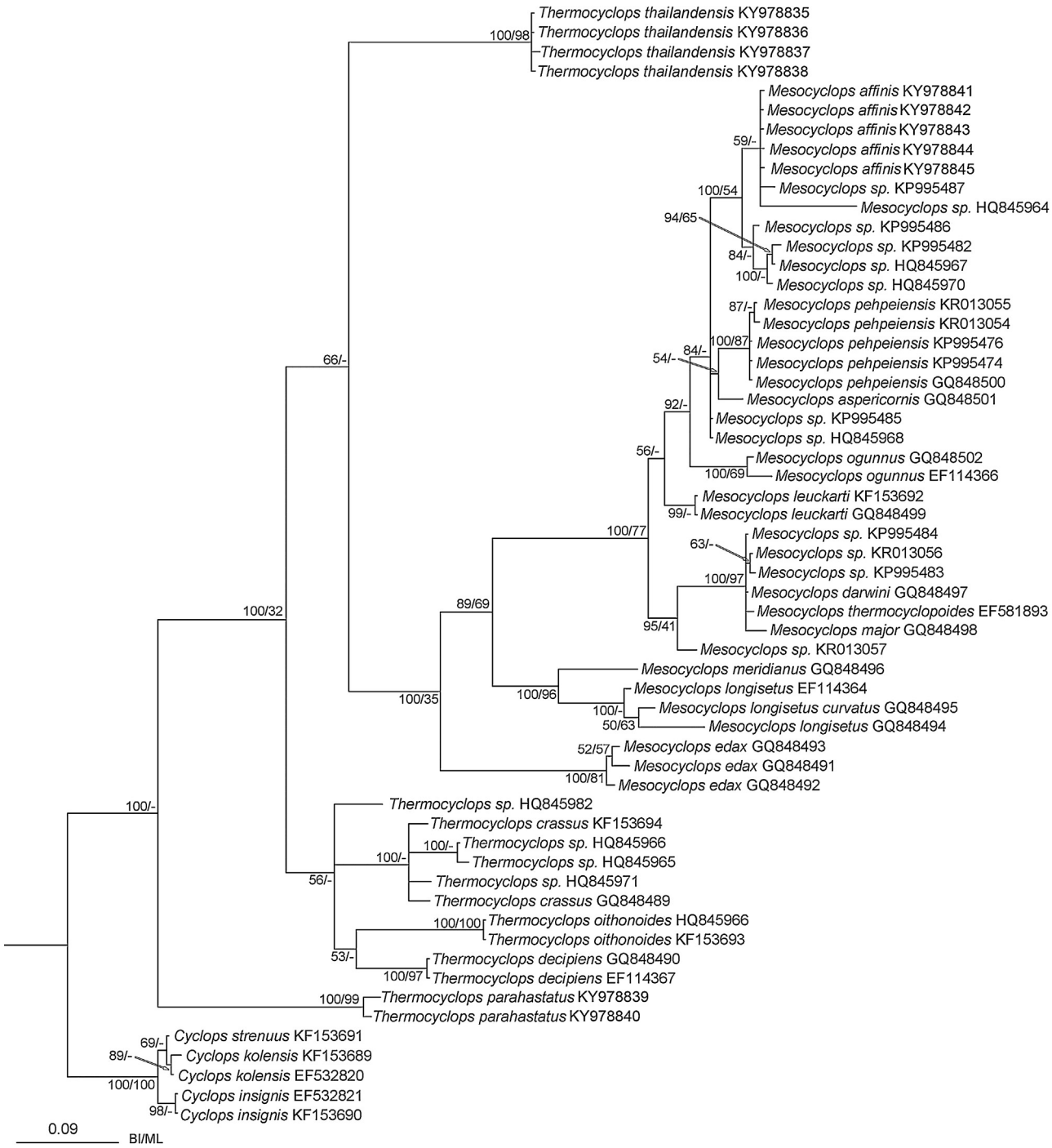

Fig. 3. Bayesian Inference (BI) tree based on ITS sequences of two specimens of *Thermocyclops parahastatus* sp. nov., four specimens of *T. thailandensis* sp. nov., five specimens of *Mesocyclops affinis* Van de Velde, 1987, and 42 other sequences from GenBank identified either as *Thermocyclps* Kiefer, 1927 or *Mesocyclops* Sars, 1914. The tree is computed using MrBayes, drawn to scale, and rooted with members of the genus *Cyclops* Müller, 1785. Numbers on the branches represent posterior probabilities in MrBuyes/bootstrap values from 1000 pseudo-replicates in MEGA 6 obtained from a maximum likelihood (ML) analysis (GTR + G + I model) of the same dataset. Codes after species names represent their GenBank accession numbers.

with five large sensilla. Cephalothorax (Fig. 4A) slightly shorter than its greatest width; represents 42% of total body length, and about 1.6 times as long as three free prosomites combined; free prosomites progressively shorter and narrower towards posterior end (Fig. 4A–C).

Genital double-somite (Figs. 4 D, E, 5 C, D, 8 B) about as long as wide in ventral view, anterior (widest) part nearly 1.4 times as wide as posterior margin; anterior part ornamented with one pair of narrowly spaced dorsal sensilla (Fig. 5C), one pair of lateral sensilla (Fig. 4D, E), large cuticular pore postero-dorsal from genital operculum (Fig. 4E), and four small pores arranged into square postero-central from genital operculum (near distal tip of inner spine; Fig. 4E); posterior part ornamented with one pair of widely spaced dorsal sensilla (Fig. 5C), one pair of lateral sensilla (Fig. 4D), one pair of lateral pores (Fig. 4D), and two pairs of ventral pores (Suppl. Fig. 1B). Medial copulatory pore (Suppl. Fig. 1B) small, ovoid, situated in first quarter. Copulatory duct short, narrow, rigidly sclerotized, directed posteriorly. Seminal receptacle

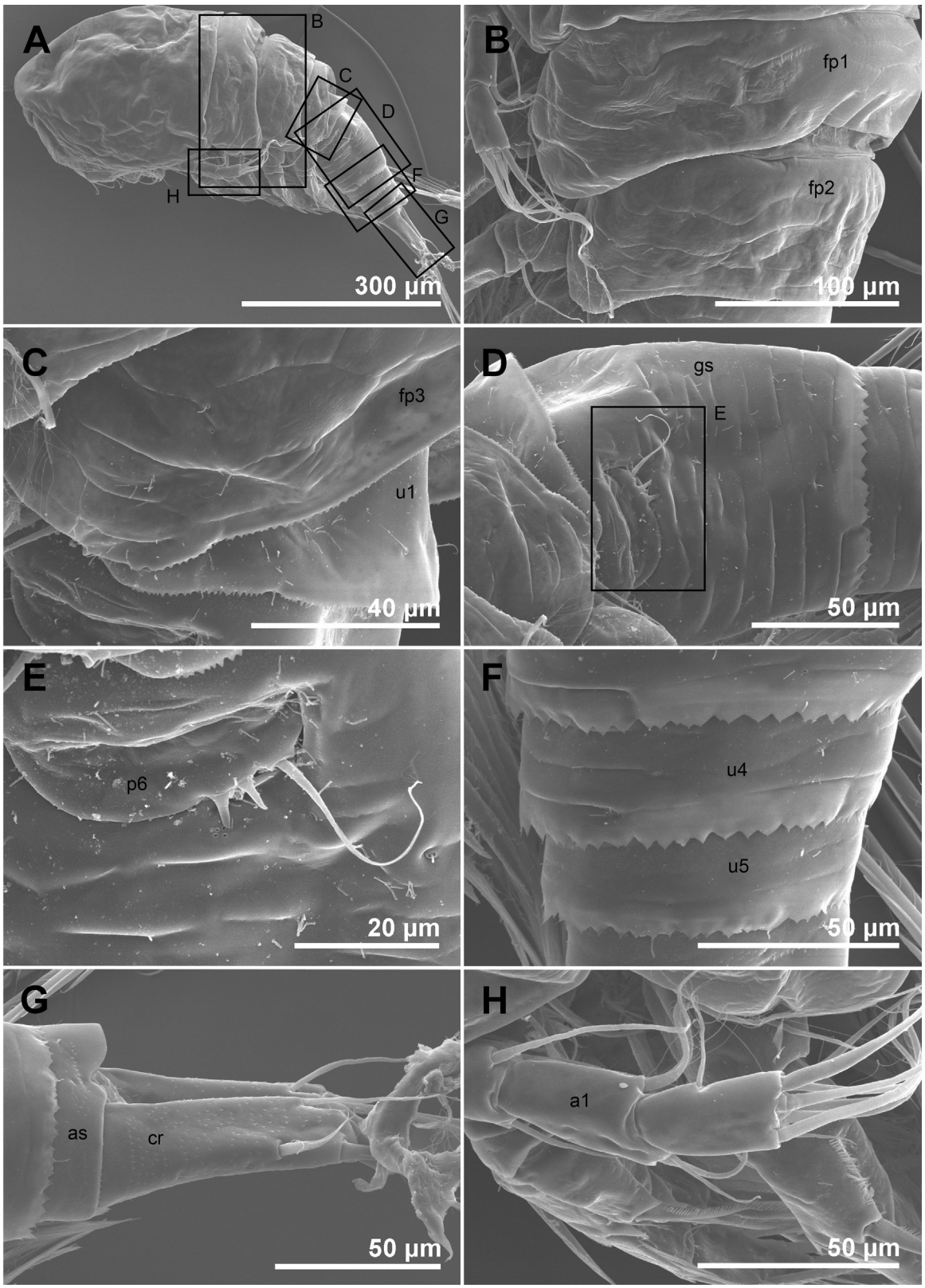

Fig. 4. *Thermocyclops parahastatus* sp. nov., SEM photographs, paratype female 1: (A) habitus, lateral, (B) first (fp1) and second (fp2) free prosomites, lateral, (C) third (fp3) free prosomite and first urosomite (u1), lateral, (D) genital double-somite (gs), lateral, (E) sixth leg (p6), anterior, (F) fourth (u4) and fifth (u5) urosomites, lateral, (G) anal somite (as) and caudal rami (cr), lateral, (H) distal part of antennula (a1), lateral. Rectangles in A and D showing areas given as close-ups in B-H.

(Suppl. Fig. 1B) relatively small, distal part ovoid, reaching three fifths of somite's length, and only slightly larger than any of posteriorly curved lateral arms. Parts of oviducts rigidly sclerotized. Ovipores situated dorsolaterally, small, covered by reduced sixth legs. Third urosomite (Figs. 4 F, 5 D, Suppl. Fig. 1B) with single widely spaced pair of dorsal sensilla and two pairs of ventral pores. Fourth

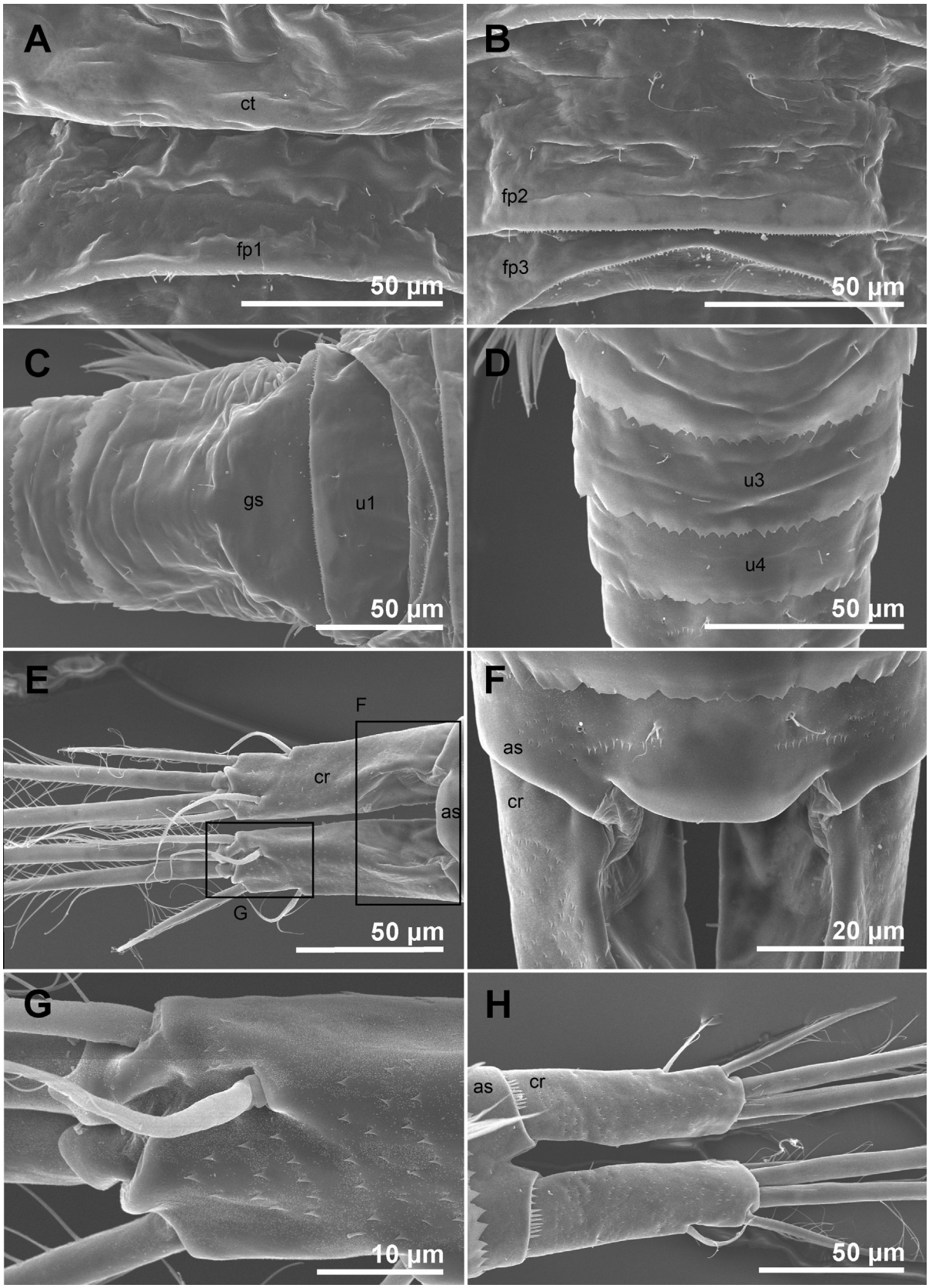

Fig. 5. *Thermocyclops parahastatus* sp. nov., SEM photographs, (A–G) paratype female 2, (H) paratype female 3: (A) medial part of cephalothorax (ct) and first free prosomite (fp1), dorsal, (B) medial part of second (fp2) and third (fp3) free prosomites, dorsal, (C) first ursomomite (u1) and gential double-somite (gs), dorsal, (D) third (u3) and fourth (u4) urosomites, dorsal, (E) anal somite (as) and caudal rami (cr), dorsal, (F) anal somite (as) and anterior part of caudal rami (cr), dorsal, (G) posterior part of caudal ramus, dorsal, (H) anal somite (as) and caudal rami (cr), ventral. Rectangles in E showing areas given as close-ups in F and G.

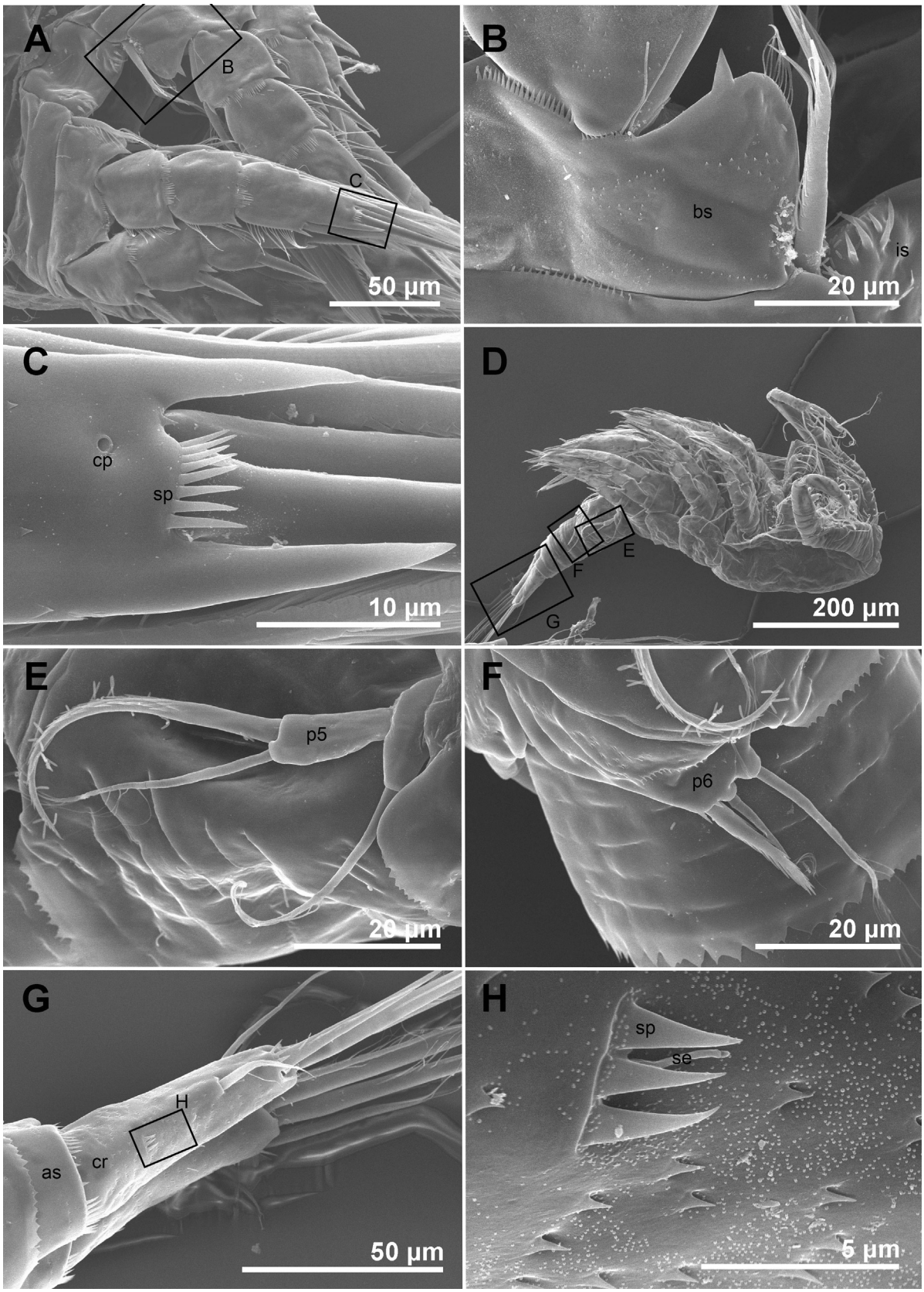

Fig. 6. *Thermocyclops parahastatus* sp. nov., SEM photographs, (A–C) paratype female 3, (D–H) paratype male 1: (A) second swimming leg, anterior, (B) basis (bs) of second swimming leg and part of intercoxal sclerite (is) with spinules, anterior, (C) distal part of third endopodal segment of second swimming leg, with cuticular pore (cp) and distal spinules (sp), anterior, (D) habitus, ventro-lateral, (E) fifth leg (p5), anterior, (F) sixth leg (p6), anterior, (G) anal somite (as) and caudal rami (cr), ventro-lateral, (H) anterior row of spinules (sp) flanking sensilla (se) on caudal ramus, ventro-lateral. Rectangles in A, D and G showing areas given as close-ups in B, C, E, F, and H.

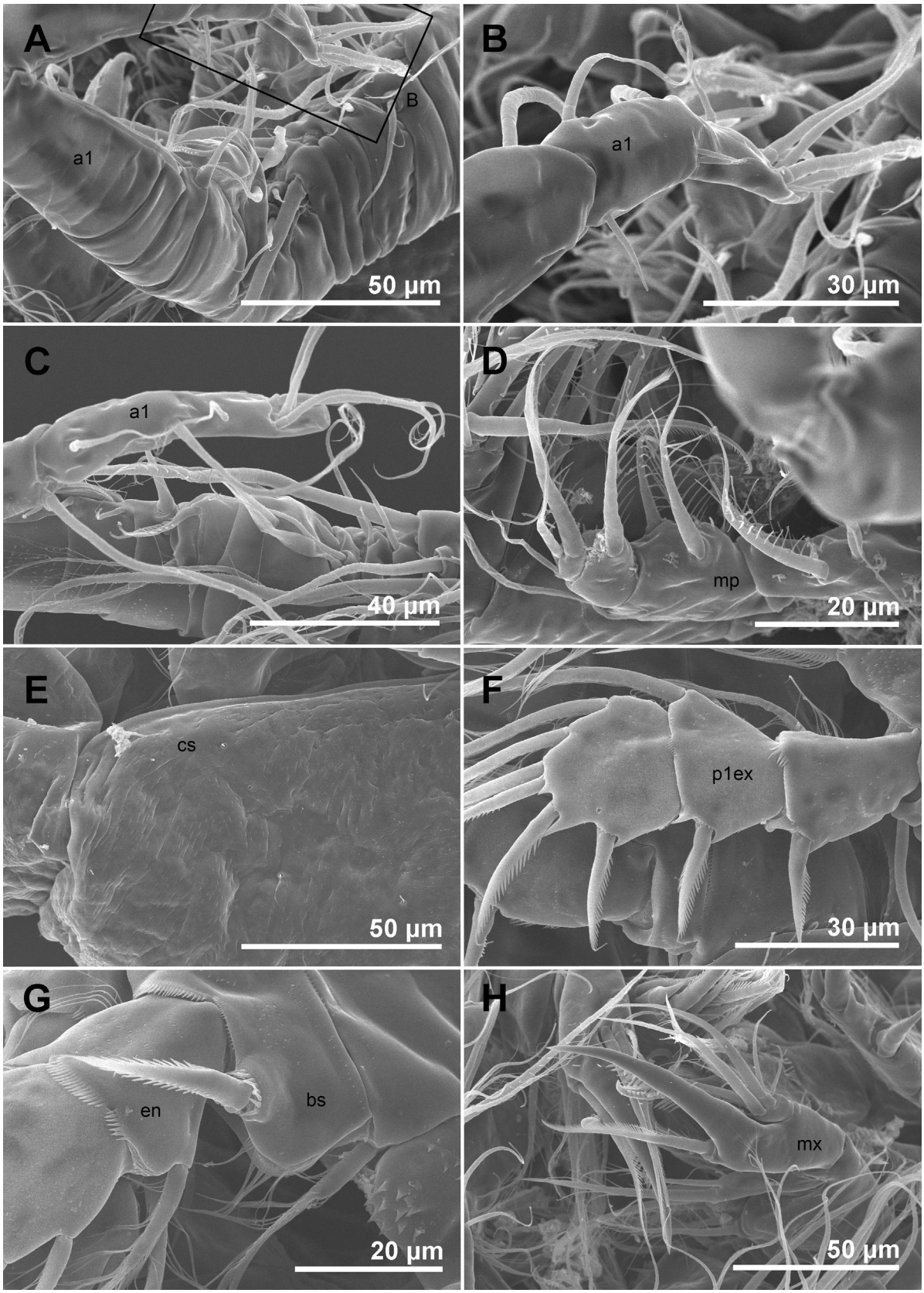

Fig. 7. *Thermocyclops parahastatus* sp. nov., SEM photographs, (A–D) paratype male 1, (E) paratype male 2, (F–G) paratype male 3, (H) paratype female 3: (A) left antennula (a1), ventro-lateral, (B) distal part of left antennula (a1), ventro-lateral, (C) right antennula (a1), ventro-lateral, (D) maxilliped (mp), ventro-lateral, (E) posterior part of cephalothoracic shield (cs), lateral, (F) exopod of first swimming leg (p1ex), anterior, (G) basis (bs) and proximal part of endopod (en) of first swimming leg, anterior, (H) maxilla (mx), ventral. A rectangle in A showing an area given as a close-up in B.

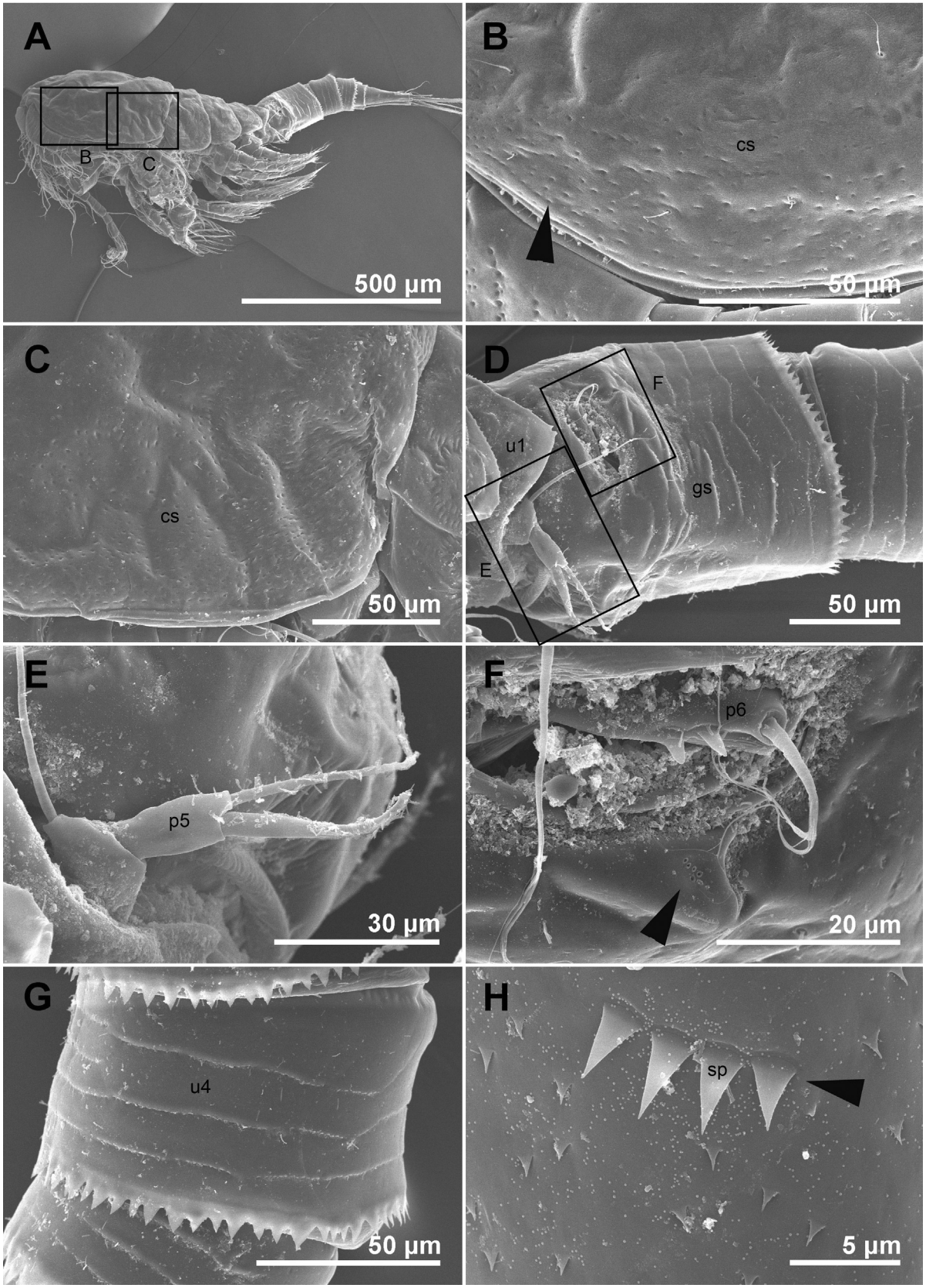

Fig. 8. *Thermocyclops thailandensis* sp. nov., SEM photographs, paratype female 1: (A) habitus, lateral, (B) anterior part of cephalothoracic shield (cs), lateral, (C) posterior part of cephalothoracic shield (cs), lateral, (D) first urosomite (u1) and genital double-somite (gs), lateral, (E) fifth leg (p5), anterior, (F) sixth leg (p6), anterior, (G) fourth urosomite u4), lateral, (H) anterior row of spinules (sp) on caudal ramus, lateral. Arrowheads indicating most prominent differences from *T. parahastatus* sp. nov. Rectangles in A and D showing areas given as close-ups in B, C, E, and F.

urosomite (Figs. 4 F, 5 D, Suppl. Fig. 1B) with single ventral pair of ventral pores. Anal somite (Figs. 4 G, 5 F, Suppl. Fig. 1B) with two large dorsal sensilla, short ventral rows of large spinules on posterior margin, numerous minute spinules on all sides, two pairs of dorsal cuticular pores, and one pair of ventral cuticular pores; anal operculum smooth, broad, long, and strongly convex, represents 48% of somite's width, and extends to posterior margin of somite; anal sinus not widely opened, without visible ornamentation.

Caudal rami (Figs. 4 G, 5 E,–H, Suppl. Fig. 1B) about three times as long as wide in ventral view, cylindrical, parallel, with space between them about half of one ramus width, ornamented with numerous minute spinules on all surfaces, except dorso-median anterior invagination that joins anal sinus, with small lateral tubular pore at first third, and ventral posterior simple pore at base of principal apical setae. All setae slender and bipinnate, and all except dorsal seta uniarticulated at base; dorsal seta about 0.7 times as long as ramus, inserted at four fifths of ramus length, biarticulated at base; lateral seta smallest, about as long as one ramus width; outermost apical seta stronger than innermost apical but not spiniform, about 0.7 times as long as ramus, and 0.8 times as long as innermost apical seta; principal apical setae with breaking planes, inner one about three times as long as caudal ramus and 1.5 times as long as outer one.

Antennula (Fig. 4H, Suppl. Fig. 2A) 17-segmented, slender, its distal tip reaching midlength of first free prosomite; single slender aesthetasc present on twelfth segment; setal formula: 8.4.2.6.6.2.2.1.1.0.1.1.0.1.2.3.8; no setae with breaking planes and only one apical seta on seventeenth segment biarticulated; all setae slender and most larger setae pinnate; first segment with short, arched row of large spinules in proximal part, sixteenth segment with serrated longitudinal frill, all other segments smooth; seventeenth segment 1.8 times as long as wide.

Antenna (Suppl. Fig. 1C) five-segmented, comprising minute coxa, well-developed basis, and three-segmented endopod; coxa unarmed and unornamented, about 2.8 times as wide as long; basis largest segment, slightly curved but generally cylindrical, about 2.2 times as long as wide, ornamented with three diagonal short rows of spinules on posterior surface, two short diagonal rows of spinules on anterior surface, and one longitudinal row of minute spinules along inner margin, armed with single smooth seta at distal inner corner and with strong pinnate seta representing exopod, which reaches beyond tip of appendage; first endopodal segment narrower proximally than distally, about 0.8 times as long as basis and 1.8 times as long as wide, armed with single smooth seta on inner margin, ornamented with longitudinal row of spinules along outer margin; second endopodal segment also slightly narrower proximally than distally, about as long as first endopodal segment but slightly more slender, twice as long as wide, ornamented with longitudinal row of spinules along outer margin, armed with six smooth setae (four lateral, two subapical) along inner margin; third endopodal segment cylindrical, slightly shorter than second endopodal segment and more slender, 2.7 times as long as wide, armed with seven apical setae, ornamented with long spinnules along outer margin.

Labrum (Suppl. Fig. 1D) trapezoidal, ornamented with two rows of eight long and slender spinules on posterior surface; cutting edge slightly concave, with 12 sharp teeth between blunt and smooth lateral corners.

Mandibula (Suppl. Figs. 2B–D) with small but distinct palp, armed with two very long, plumose setae and one short, smooth, seta; coxal gnathobase cutting edge relatively narrow, with one quadricuspidate tooth on ventral margin, two pinnate setae on dorsal margin, and in between three bicuspidate teeth, two unicuspidate teeth, and one row of seven slender spinules on anterior surface; dorsalmot seta on cutting edge bipinnate, about twice as long as other, unipinnate seta on cutting edge, and 1.4 times as long as smooth palpal seta.

Maxillula (Suppl. Fig. 1E, F) composed of well-developed praecoxa and two-segmented palp; arthrite of praecoxa with four strong apical spines, three of them smooth and fused to arthrite basally, one articulated and unipinnate; praecoxa armed with eight armature elements along inner margin, longest one plumose; palp (Suppl. Fig. 1F) somewhat shorter than arthrite of praecoxa, composed of ovoid basis and minute but distinct endopod, exopod reduced to minute bump bearing single seta; basis smooth, about 1.7 times as long as wide and five times as long as endopod, armed with one spiniform and two slender setae on inner margin; endopod smooth, slightly wider than long, armed with one inner and two apical slender, pinnate setae.

Maxilla (Fig. 7H, Suppl. Fig. 2E) unornamented, composed of preacoxa, coxa, basis, and two-segmented endopod; praecoxa fused to coxa on anterior surface; praecoxa smooth, wider than long, with two endites, proximal endite armed with two pinnate setae, distal endite small and unarmed; coxa with several transverse striae along outer surface, longer than wide and longer than praecoxa, with two endites, proximal endite minute, armed with single bipinnate seta, distal endite large and highly mobile, more than twice as long as wide, armed with two pinnate setae, proximal seta about 1.5 times as long as distal seta and nearly four times as long as distal endite; basis smooth, half as long as coxa, expanded into robust claw and armed with two additional articulated setae, claw with longitudinal row of 12–14 strong spinules along concave margin, proximal seta strong, bipinnate, slightly longer than claw and about 1.6 times as long as distal smooth seta; endopod minute, smooth, first segment much larger than second segment and 2.6 times as long, armed with one robust and one slender seta, second segment armed with one robust and two slender setae; robust seta on first endopodal segment 1.2 times as long as robust seta on second endopodal segment or basal claw.

Maxilliped (Suppl. Fig. 2F) four-segmented, composed of syncoxa, basis, and two-segmented endopod; syncoxa cylindrical, 1.4 times as long as wide, ornamented with one field of spinules on anterior surface near proximal-outer corner, armed with three inner pinnate setae of similar lengths; basis roughly pentagonal, 1.5 times as long as wide, 0.8 times as long as syncoxa, ornamented with one large field of spinules on posterior surface and two transverse rows of spinules on posterior surface, armed with two bipinnate setae, proximal seta 1.8 times as long as distal one; first endopodal segment ovoid, only 0.3 times as long as basis, ornamented with one arched row of spinules on posterior surface, armed with single strong, unipinnate seta; second endopodal segment triangular, minute, less than half as long as first endopodal segment, unornamented, armed with one unipinnate and two smooth setae; only seta on second endopodal segment longest, about 1.2 times as long as robust seta on basis or second endopodal segment.

Swimming legs (Fig. 6A–C, Suppl. Fig. 3A–F) segmentation and armature formula conform to conservative generic pattern, each leg composed of coxa, basis, three-segmented exopod, three-segmented endopod, and coxae of opposite appendages connected with intercoxal sclerite; armature formula same as in, for example, *Thermocyclops aberrans* Lindberg (1952) (see Karanovic, 2006); all segments of all legs with dense pattern of minute spinules on anterior surface (see Fig. 6B); third exopodal and endopodal segments in all legs, except first leg endopod, with distal cuticular pore on anterior surface (see Fig. 6C), additional pore present near outer margin of basis and near inner margin of coxa (see Suppl. Fig. 3F); all segments with at least one posterior row of large spinules on anterior surface and endopodal segments also with large spinules along outer margin (see Fig. 6A, Suppl. Fig. 3F); intercoxal sclerites of all legs with very slightly concave distal margin, lateral promi-

nences not protruding beyond distal margin, and at least posterior row of strong spinules on anterior surface of prominences (Fig. 6B), that of the fourth leg with one additional interrupted row of spinules on anterior surface and two uninterrupted rows of spinules on posterior surface (Suppl. Fig. 3F).

Third endopodal segment of first swimming leg (Suppl. Fig. 3A) 1.4 times as long as wide, with only outer apical spiniform process, apical spine about 1.4 times as long as segment (without spiniform process). Inner spine on basis inserted well away from inner margin, distal tip of inner spine reaching distal margin of first endopodal segment.

Third endopodal segment of second swimming leg (Fig. 6A, C, Suppl. Fig. 3B) 1.7 times as long as wide, with two apical spiniform processes, apical spine about 1.1 times as long as segment. Third exopodal segment of second swimming leg (Fig. 6A, Suppl. Fig. 3C) 1.3 times as long as wide, apical spine 1.8 times as long as middle spine and 1.3 times as long as segment.

Third endopodal segment of third swimming leg (Suppl. Fig. 3D) 1.8 times as long as wide, with two apical spiniform processes, apical spine less than 1.1 times as long as segment. Third exopodal segment of third swimming leg (Suppl. Fig. 3E) 1.5 times as long as wide, apical spine 1.8 times as long as middle spine and 1.3 times as long as segment.

Third endopodal segment of fourth swimming leg (Suppl. Fig. 3F) 2.4 times as long as wide, with two apical spiniform processes and two apical spines, outer apical spine 0.9 times as long as segment and 1.2 times as long as inner spine. Third exopodal segment of fourth swimming leg (Suppl. Fig. 3E) 1.8 times as long as wide, apical spine 1.8 times as long as middle spine and 1.1 times as long as segment. Coxa of fourth swimming leg (Suppl. Fig. 3F) with five rows of large spinules on posterior surface and three rows of large spinules on anterior surface, in addition to abovementioned large spinules along distal margin and minute spinules (mostly close to outer margin); inner seta spiniform, unipinnate, 1.2 times as long as coxa, distal tip of seta reaching slightly beyond inner spiniform process of basis. Basis of fourth swimming leg (Suppl. Fig. 3F) with convex inner margin, only several spinules along posterior part of inner margin, and small, sharp spiniform process distinct from blunt inner-distal corner; distal tip of outer seta reaching distal margin of first exopodal segment. First endopodal segment of fourth leg (Suppl. Fig. 3F) with convex inner margin.

Fifth leg (Suppl. Fig. 4A) small, two-segmented, unornamented, with membranous joint with fifth pedigerous somite; first segment almost twice as wide as long, armed with lateral unipinnate seta inserted on elongated setophore; second segment much narrower, about twice as long as wide, armed apically with inner spine and outer seta, inner spine 1.3 times as long as outer seta and 2.8 times as long as segment.

Sixth leg (Fig. 4E) simple semilunar cuticular plate, 3.8 times as wide as long, unornamented, armed with two almost equally long minute smooth spines and one much longer smooth and slender seta; seta more than three times as long as plate and nearly eight times as long as spines.

3.2.1.5. Description of male. Based on five paratypes. Body length from 525 to 575 μm. Habitus (Fig. 6D) less robust in lateral view than in female, with prosome/urosome ratio 1.7, but otherwise with little observable sexual dimorphism in segmentation, proportions, posterior hyaline fringes of somites, and surface ornamentation, except genital and third urosomites not fused (Fig. 6F). Cephalothoracic shield (Fig. 7E) with more striae than in female, and even with several cuticular pits. Urosomal striae (Fig. 6D–F) about as frequent as in female.

Caudal rami (Fig. 6G, H) similar to those in female, but lateral tubular pore protected with three large spinules.

Antennula (Figs. 6 D, 7 A–C, Suppl. Fig. 4B, C) longer and more robust than in female in comparison to cephalothorax, strongly bigeniculate, 14-segmented, with proximal geniculation between eighth and ninth segments, and distal geniculation between twelfth and thirteenth segments; armature formula (ae = aeshetasc): 8 + 3ae.4.2.2.2.2 + ae.2.4 + ae.4.2.2 + ae.2.1.13; twelfth and thirteenth segments with strong cuticular ridges along anterior (geniculating) surface, each with central cuticular pore.

Antenna, labrum, mandibula, maxillula, maxilla, maxilliped (Fig. 7D), swimming legs (Figs. 7 F, G, 11 D), and fifth leg (Fig. 6E, Suppl. Fig. 4E) as in female.

Sixth leg (Fig. 6F, Suppl. Fig. 4F) simple semilunar cuticular plate as in female, but larger in proportion to somite, 2.4 times as wide as long, ornamented with several minute spinules on anterior surface, and armed with two setae and innermost spine; outermost seta 2.6 times as long as central seta, 1.8 times as long as spine, and 2.1 times as long as plate.

3.2.1.6. Variability. Except from different overall length of specimens, mostly resulting from different contractions of their telescopic somites, very few characters were observed with obviously variable features between different specimens. However, we did not perform exact morphometric analysis of any structure. Asymmetries were more common, and they mostly involved presence/absence of sensilla or pores on one side of the body (Fig. 5A) or their relative positions (Fig. 5B). Our survey of cuticular organs was not comprehensive, so more variability might be discovered in the future. We paid special attention to characters used for species delineation in this genus (genital somite, caudal rami, fourth leg), while others were compared with less rigor.

3.2.2. Thermocyclops thailandensis sp. nov. (Figs. 8–11 and Suppl. Figs. 5–8)

3.2.2.1. Type locality. Northern Thailand, Phayao Province, Ban Tham village, Tham Chom Sin cave, pool on muddy floor filled with percolating water; coordinates of the cave entrance 19°04′52.68″N 100°04′24.74″E, 443 m above sea level.

3.2.2.2. Type material. Holotype: ovigerous female dissected on one slide (WAM C55915), collected from the type locality on 10 June 2016. Paratypes: two males and three females dissected on one slide each (WAM C55916–C55920), collected from the type locality on 10 June 2016; one male and 5 females together in one alcohol vial (WAM C55921), collected from the type locality on 10 June 2016; six males and seven females together on one SEM stub (WAM C55922), collected from the type locality on 5 April 2015; eight males and 21 females together in one alcohol vial (WAM C55923), collected from the type locality on 7 December 2014.

3.2.2.3. Etymology. The species name refers to Thailand. It is an adjective for place, made with the Latin suffix "-ensis"

3.2.2.4. Description of female. Based on holotype and ten paratypes. Body length, excluding caudal setae, ranging from 870 to 998 μm. Habitus (Figs. 8 A, 10 A) slender in lateral view, with prosome/urosome ratio 1.5, and greatest width near posterior end of cephalothorax. Body length/width ratio about 2.8, cephalothorax 2.4 times as wide as genital double-somite. Free pedigerous somites without pronounced lateral expansions. Colour of preserved specimens yellowish and nauplius eye not visible. Integument (Figs. 8–10) on all somites relatively smooth, with numerous cuticular pits on cephalothorax (Fig. 8B, C; arrowed in Fig. 8B), fewer cuticular pits on free prosomites (Suppl. Fig. 5A, B) and urosomites (Fig. 8D, G, Suppl. Fig. 5C), where they generally combine into rows become similar to striae, with spinules only on anal somite and caudal rami (Figs. 8 H, 9 F, G, 10 E–G, Suppl. Fig. 5C), with irregular but mostly transverse short striae on urosomites (especially frequent on genital double-somite; see Fig. 8D, Suppl. Fig. 5C), with

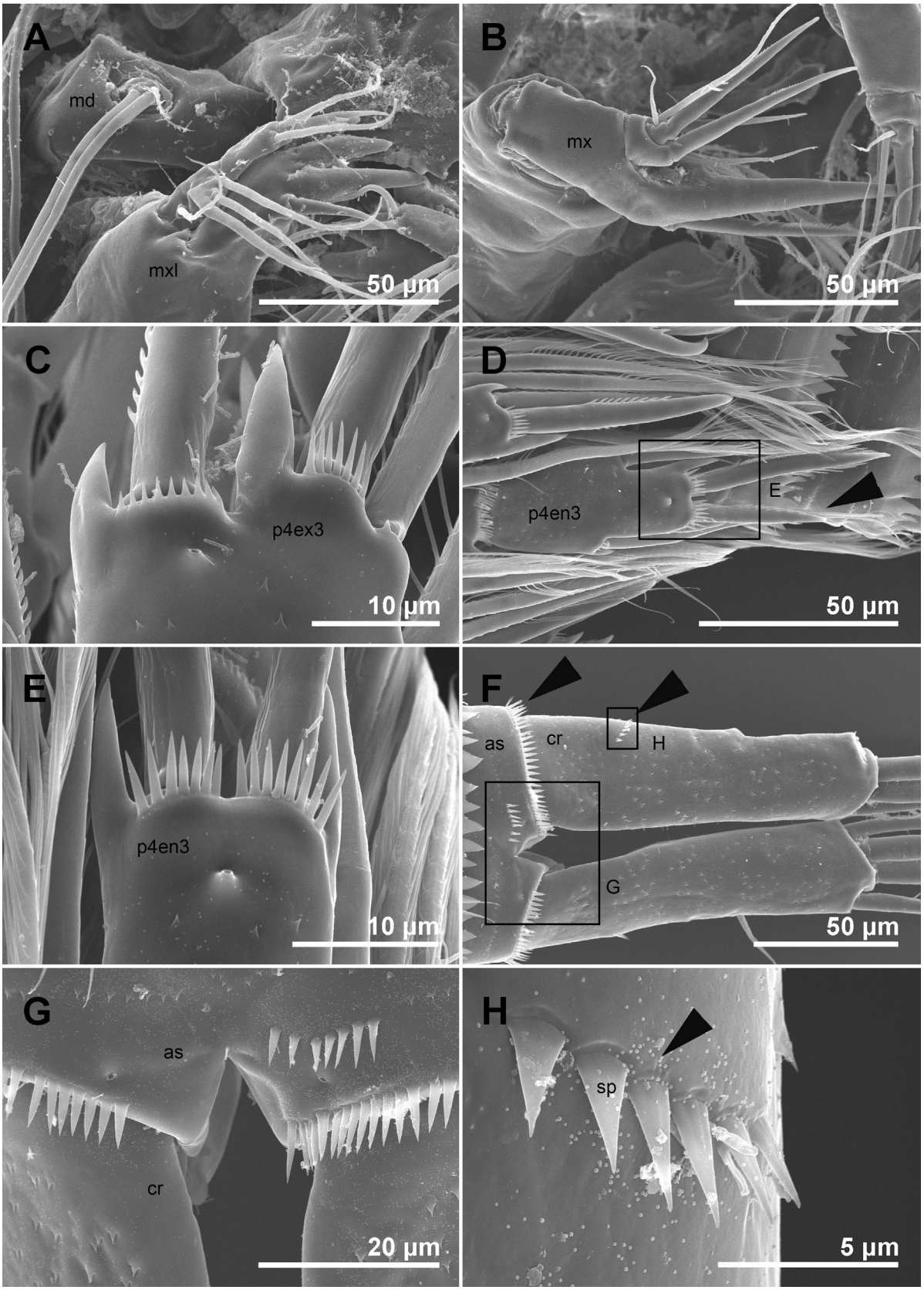

Fig. 9. *Thermocyclops thailandensis* sp. nov., SEM photographs, (A–B) paratype female 2, (C—H), paratype female 4: (A) mandibula (md) and maxillula (mxl), ventral, (B) maxilla (mx), ventral, (C) distal tip of third exopodal segment of third swimming leg (p4ex3), anterior, (D) third endopodal segment of fourth swimming leg (p4en3), anterior, (E) distal tip of third endopodal segment of fourth swimming leg (p4en3), anterior, (F) anal somite (as) and caudal rami (cr), ventral, (G) part of anal somite (as) and base of caudal rami (cr), ventral, (H) anterior row of spinules (sp) on caudal rami, ventral. Arrowheads indicating most prominent differences from *T. parahastatus* sp. nov. Rectangles in D and F showing areas given as close-ups in E, G, and H.

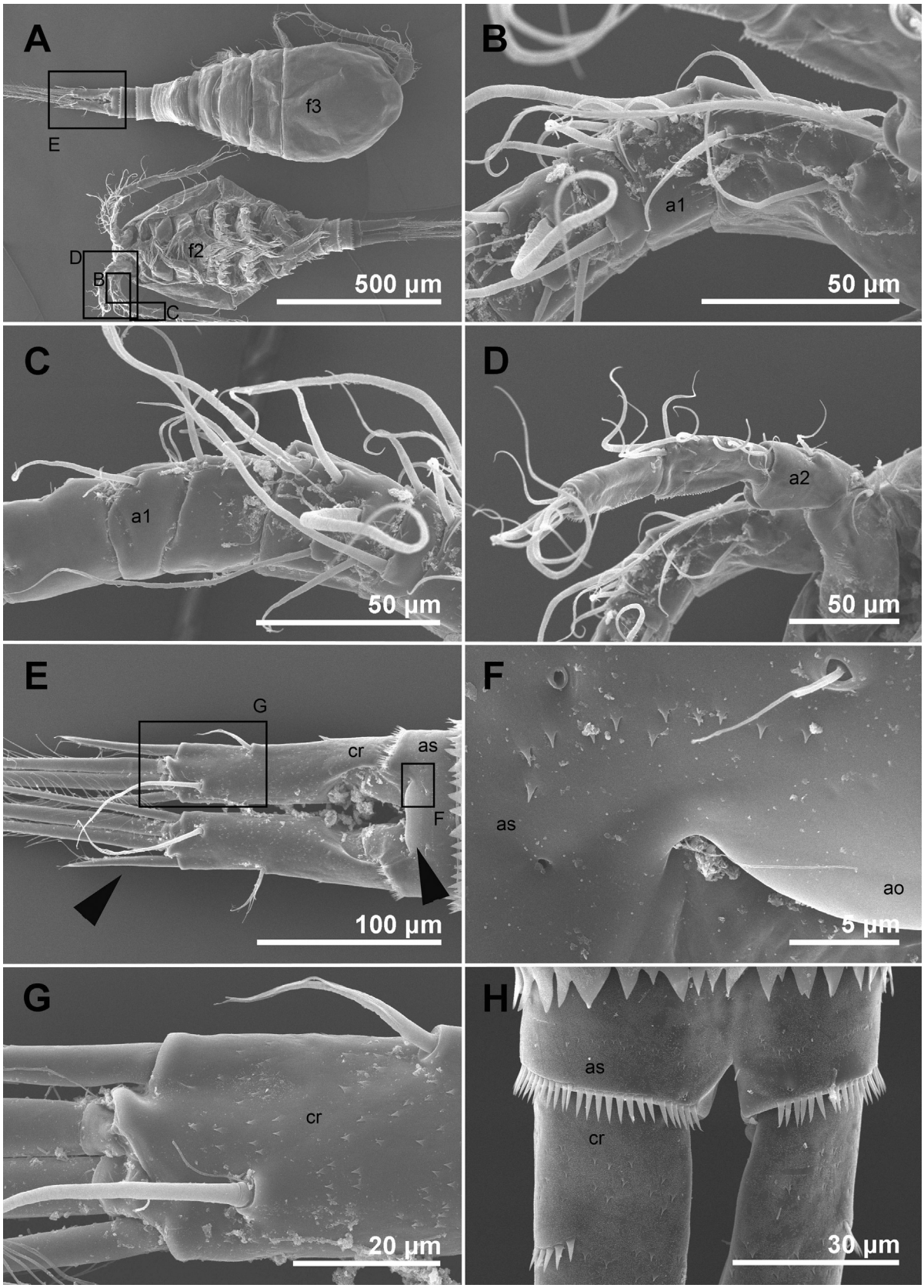

Fig. 10. *Thermocyclops thailandensis* sp. nov., SEM photographs, (A) paratype females 2 (ventral) and 3 (dorsal) (f2 and f3 respectively), (B–D), paratype female 2, (E–G) paratype female 3, (H) paratype male 1: (A) habitus, dorsal and ventral, (B) proximal part of antennula (a1), ventral, (C) central part of antennula (a1), ventral, (D) antenna (a2), ventral, (E) anal somite (as) and caudal rami (cr), dorsal, (F) part of anal operculum (ao) and ornamentation of anal somite (as), dorsal, (G) distal part of caudal ramus (cr), dorsal, (H) anal somite (as) and anterior part of caudal rami (cr), ventral. Arrowheads indicating most prominent differences from *T. parahastatus* sp. nov. Rectangles in A and E showing areas given as close-ups in B-G.

cuticular pores and sensilla on all but penultimate somite. Posterior hyaline fringes of cephalothorax (Fig. 8C) and first two free prosomites (Suppl. Fig. 5A, B) smooth, those of third prosomite and first urosomite finely serrated (Fig. 8D), those of other urosomites (except anal somite) coarsely serrated (Fig. 8D, G, Suppl. Fig. 5C). Rostrum well-developed, membranous, very broad, and sensilla pattern not observed. Cephalothorax (Fig. 8A–C, Fig. 10) about as long as wide in dorsal view; represents 36% of total body length, and about 1.5 times as long as three free prosomites combined; free prosomites progressively shorter and narrower towards posterior end and bearing less sensilla (Suppl. Fig. 5A, B).

Genital double-somite (Fig. 8D–F, Suppl. Fig. 5C) about 0.8 times as long as wide in ventral view, anterior part 1.3 times as wide as posterior margin; anterior part ornamented with one pair of narrowly spaced dorsal sensilla (Fig. 8D), one pair of lateral sensilla (Fig. 8F), and five small pores arranged into L-shape posterior from genital operculum (near distal tip of inner spine; arrowed in Fig. 8F); posterior part ornamented with one pair of widely spaced dorsal sensilla (Fig. 8D), one pair of lateral sensilla (Fig. 8D), one pair of lateral pores (Fig. 8D), and one pair of ventral pores (Suppl. Fig. 5C). Medial copulatory pore (Suppl. Fig. 5C) minute, situated in first quarter. Copulatory duct short, narrow, rigidly sclerotized, directed anteriorly. Seminal receptacle relatively large (Suppl. Fig. 5C), distal part cylindrical, reaching four fifths of somite's length (arrowed in Suppl. Fig. 5C), and significantly larger than any of slightly posteriorly curved lateral arms. Parts of oviducts and anterior margin of lateral arms rigidly sclerotized (arrowed in Suppl. Fig. 5C). Ovipores situated dorsolaterally, relatively small, covered by reduced sixth legs. Third urosomite (Fig. 8G, Suppl. Fig. 5C) with single widely spaced pair of dorsal sensilla, one pair of lateral sensilla, and one pair of ventral pores. Fourth urosomite (Suppl. Fig. 5C) without sensilla or pores, about 0.8 times as long as third urosomite. Anal somite (Figs. 9 F, G, 10 E, F, Suppl. Fig. 5C) with two large dorsal sensilla, long ventral rows of large spinules on posterior margin (arrowed in Fig. 9F), many minute spinules on all sides, two pairs of dorsal cuticular pores, one pair of ventral cuticular pores, and sometimes with several large spinules at base of ventral pores (see Fig. 9G); anal operculum smooth, broad, short (arrowed in Fig. 10E), and nearly straight, represents 43% of somite's width, not reaching posterior margin of somite; anal sinus (Fig. 10E) widely opened, smooth.

Caudal rami (Figs. 8 H, 9 F, G, H, 10 E, G, Suppl. Fig. 5C) about 3.9 times as long as wide in ventral view, cylindrical, parallel, with space between them about half of one ramus width, ornamented with numerous minute spinules on all surfaces, except dorsomedian anterior invagination that joins anal sinus, with small lateral tubular pore at first third protected with row of spinules (arrowed in Figs. 8 H, 9 F, H, Suppl. Fig. 5C), and ventral posterior simple pore at base of principal apical setae. Outermost apical seta spiniform (arrowed in Fig. 10E, Suppl. Fig. 5C), all other setae slender and pinnate, and all except dorsal seta uniarticulated at base; dorsal seta about 0.6 times as long as ramus, inserted at four fifths of ramus length, biarticulated at base; lateral seta smallest, about 0.7 times as long as one ramus width; outermost apical seta significantly stronger than innermost apical, about half as long as ramus, and 0.3 times as long as innermost apical seta (arrowed in Suppl. Fig. 5C); principal apical setae with breaking planes, inner one about three times as long as caudal ramus and 1.6 times as long as outer one.

Antennula (Figs. 8 A, 10 A–C, Suppl. Fig. 6A, B) 17-segmented, slender, its distal tip reaching midlength of first free prosomite; single slender aesthetasc present on twelfth segment; setal formula: 8.4.2.6.5.2.2.1.1.0.1.1.0.1.2.3.8 (one less seta on fifth segment arrowed in Suppl. Fig. 6A); no setae with breaking planes and only one apical seta on seventeenth segment biarticulated; all setae slender and most larger setae pinnate; first segment with short, arched row of large spinules in proximal part, and several rows of cuticular pits, all other segments smooth (i.e. sixteenth segment without serrated longitudinal frill); seventeenth segment 2.4 times as long as wide (arrowed in Suppl. Fig. 6B).

Antenna (Fig. 10D, Suppl. Fig. 5D) five-segmented, comprising minute coxa, well-developed basis, and three-segmented endopod; coxa unarmed and unornamented, about twice as wide as long; basis largest segment, slightly curved but generally cylindrical, about 2.1 times as long as wide, ornamented with three diagonal short rows of spinules on posterior surface, one row of spinules on anterior surface, and one short longitudinal row of minute spinules along proximal part of inner margin, armed two smooth setae at distal inner corner (arrowed in Suppl. Fig. 5D) and with strong pinnate seta representing exopod, which nearly reaches tip of appendage; first endopodal segment slightly narrower proximally than distally, about 0.8 times as long as basis and 1.8 times as long as wide, armed with single smooth seta on inner margin, ornamented with longitudinal row of spinules along outer margin; second endopodal segment also slightly narrower proximally than distally, about as long as first endopodal segment but slightly more slender, 2.2 times as long as wide, ornamented with longitudinal row of spinules along outer margin, armed with nine smooth setae (seven lateral, two subapical) along inner margin (arrowed in Suppl. Fig. 5D); third endopodal segment cylindrical, as longas second endopodal segment but more slender, 3.2 times as long as wide, armed with seven apical setae, ornamented with short spinnules along outer margin.

Labrum (Fig. 9A, Suppl. Fig. 5E) trapezoidal, ornamented with two rows of eight long and slender spinules on posterior surface and two pores on anterior surface; cutting edge slightly concave, with 10 sharp teeth (arrowed in Suppl. Fig. 5E) between blunt and smooth lateral corners.

Paragnaths (Suppl. Fig. 6C) thumb-like, with rigidly sclerotized distal part and membraneous, borad base, ornamented with three strong basal teeth and two parallel rows of distal spinules.

Mandibula (Fig. 9A, Suppl. Fig. 6) with small but distinct palp, armed with two very long, plumose setae and one short, smooth, seta; coxal gnathobase cutting edge relatively narrow, with one quadricuspidate tooth on ventral margin (dorsalmost cusp longest; arrowed in Suppl. Fig. 6E), two pinnate setae on dorsal margin, and in between three bicuspidate teeth, two unicuspidate teeth, and one row of five slender spinules on anterior surface; dorsalmot seta on cutting edge unipinnate, about 1.4 times as long as other, spiniform seta on cutting edge, and about as long as smooth palpal seta.

Maxillula (Fig. 9A, Suppl. Fig. 6F, G) composed of well-developed praecoxa and two-segmented palp; arthrite of praecoxa (Suppl. Fig. 6F) with four strong and smooth apical spines, three of them fused to arthrite basally, one articulated; praecoxa (Suppl. Fig. 6F) armed with seven armature elements along inner margin, longest one plumose; palp (Suppl. Fig. 6G) somewhat shorter than arthrite of praecoxa, composed of cylindrical basis and small but distinct endopod, exopod reduced to minute bump bearing single seta; basis smooth, about three times as long as wide and 3.5 times as long as endopod, armed with one spiniform and two slender setae on inner margin; endopod smooth, about as wide as long (arrowed in Suppl. Fig. 6G), armed with one inner and two apical slender, pinnate setae.

Maxilla (Fig. 9B, Suppl. Fig. 6H) unornamented, composed of preacoxa, coxa, basis, and two-segmented endopod; praecoxa fused to coxa on anterior surface; praecoxa smooth, wider than long, with two endites, proximal endite armed with two pinnate setae, distal endite small and unarmed; coxa with several transverse striae and cuticular pits along outer surface, longer than wide and longer than praecoxa, with two endites, proximal endite minute, armed with single bipinnate seta, distal endite large and

highly mobile, more than twice as long as wide, armed with two pinnate setae; basis smooth, half as long as coxa, expanded into robust claw and armed with two additional articulated setae, claw with longitudinal row of 12–14 strong spinules along concave margin, proximal seta strong, bipinnate, slightly shorter than claw and about 1.8 times as long as distal smooth seta; endopod minute, smooth, first segment twice as wide as second segment and 1.4 times as long, armed with two robust setae, second segment armed with one robust and two slender setae; longer seta on first endopodal segment 1.2 times as long as robust seta on second endopodal segment but significantly shorter than basal claw (arrowed in Suppl. Fig. 6H).

Maxilliped (Suppl. Fig. 6I) four-segmented, composed of syncoxa, basis, and two-segmented endopod; syncoxa cylindrical, 2.1 times as long as wide, ornamented with one arched row of spinules on anterior surface near proximal-outer corner, armed with three inner pinnate setae, central one longest; basis roughly pentagonal, nearly twice times as long as wide (arrowed in Suppl. Fig. 6I), 0.8 times as long as syncoxa, ornamented with two arched rows of spinules on posterior surface and one arched row of spinules on posterior surface, armed with two pinnate setae, proximal seta 1.5 times as long as distal one; first endopodal segment ovoid, only 0.3 times as long as basis, unornamented, armed with single strong, bipinnate seta; second endopodal segment also ovoid, minute, less than half as long as first endopodal segment, unornamented, armed with one unipinnate and two smooth setae; strong setae on first and second endopodal segment of about same length, shape and with similar ornamentation.

Swimming legs (Figs. 9C, D, E, Suppl. Figs. 7A–E) segmentation and armature formula same as in *T. parahastatus* (see above) or *T. aberrans* (see Karanovic 2006); all segments of all legs with dense pattern of minute spinules on anterior surface (see Fig. 6B); third exopodal and endopodal segments in all legs, except first leg endopod, with distal cuticular pore on anterior surface (see Fig. 9C–E), additional pore present near outer margin of basis and near inner margin of coxa (see Suppl. Fig. 7E); all segments with at least one posterior row of large spinules on anterior surface and endopodal segments also with large spinules along outer margin (see Suppl. Fig. 7E); intercoxal sclerites of all legs smooth, with very slightly concave distal margin but lateral blunt prominences protruding well beyond distal margin (arrowed in Suppl. Fig. 7E).

Third endopodal segment of first swimming leg (Suppl. Fig. 7C) 1.2 times as long as wide (arrowed in Suppl. Fig. 7C), with only outer apical spiniform process, apical spine about 1.2 times as long as segment (without spiniform process). Inner spine on basis inserted very close to inner margin (arrowed in Suppl. Fig. 7), distal tip of inner spine reaching significantly beyond distal margin of first endopodal segment.

Second swimming leg similar to that in *T. parahastatus*, except for smooth intercoxal sclerite and spiniform basal processes closer to inner margin.

Third endopodal segment of third swimming leg (Suppl. Fig. 8C) 1.7 times as long as wide, with two apical spiniform processes, apical spine less than 1.1 times as long as segment. Third exopodal segment of third swimming leg (Fig. 9C, Suppl. Fig. 8B) 1.4 times as long as wide, apical spine 1.8 times as long as middle spine and 1.2 times as long as segment.

Third endopodal segment of fourth swimming leg (Figs. 9D, E, Suppl. Fig. 7E) 2.3 times as long as wide, with two apical spiniform processes and two apical spines, outer apical spine 0.7 times as long as segment and 0.8 times as long as inner spine (arrowed in Fig. 9D, Suppl. Fig. 7E). Third exopodal segment of fourth swimming leg (Suppl. Fig. 7E) 1.7 times as long as wide, apical spine 1.7 times as long as middle spine and 0.9 times as long as segment. Coxa of fourth swimming leg (Suppl. Fig. 7E) with three transverse rows of large spinules on posterior surface and one longitudinal row of large spinules on anterior surface, in addition to above-mentioned large spinules along distal margin and minute spinules; inner seta plumose, 1.2 times as long as coxa, distal tip of seta reaching beyond inner spiniform process of basis. Basis of fourth swimming leg (Suppl. Fig. 7E) with straight and smooth inner margin and large spiniform process as continuation of inner margin (arrowed in Suppl. Fig. 7E); distal tip of outer seta not reaching distal margin of first exopodal segment. First endopodal segment of fourth leg with concave inner margin (arrowed in Suppl. Fig. 7E).

Fifth leg (Fig. 8E, Suppl. Fig. 8D) small, two-segmented, unornamented; first segment about 1.5 times as wide as long, armed with lateral unipinnate seta inserted on short setophore; second segment much narrower, about twice as long as wide, armed apically with inner spine and outer seta, inner spine 0.7 times as long as outer seta (arrowed in Suppl. Fig. 8D) and 2.7 times as long as segment.

Sixth leg (Fig. 8F) similar in shape, ornamentation, and armature to that in *T. parahastatus*, but both spines smaller and seta clearly plumose.

3.2.2.5. Description of male. Based on eight paratypes. Body length from 695 to 731 μm. Habitus (Fig. 11G) about as robust in lateral view as in female, with prosome/urosome ratio 1.5, but otherwise with little observable sexual dimorphism in segmentation, proportions, posterior hyaline fringes of somites, and surface ornamentation, except genital and third urosomal somites not fused (Fig. 11E, F).

Caudal rami (Fig. 10H) similar to those in female, with lateral tubular pore protected with several large spinules.

Antennula (Figs. 11A–H, Suppl. Fig. 8A) similar to that in *T. parahastatus* (see above), but twelfth and fourteenth segments subdivided (both arrowed in Suppl. Fig. 8A), additional aesthetasc present on thirteenth segment (arrowed in Suppl. Fig. 8A), one less seta on eighth segment, and no spinules on first segment.

Antenna, labrum, paragnaths, mandibula, maxillula, maxilla, maxilliped, swimming legs (smooth intercoxal sclerite with lateral blunt prominences protruding well beyond distal margin arrowed in Fig. 11D), and fifth leg as in female.

Sixth leg (Fig. 11E) similar to that in *T. parahastatus* (see above), but inner spine more robust and longer.

3.2.2.6. Variability. Anal somite can be with (Figs. 9F, G) or without (Fig. 10H, Suppl. Fig. 5C) large spinules at the base of ventral pores, and this can be even asymmetrical

4. Discussion

Morphological analysis of the two new species of *Thermocyclops* confirmed our molecular results, which suggested them as being only remotely related. This probably translates into different biology and behaviour, and could explain their sympatry in the Tham Chom Sin cave on all three sampling occasions. Distinguishing morphological characters between them are numerous and here we will mention only a few major ones: ornamentation of the cephalothorax (smooth in *T. parahastatus* vs. pitted in *T. thailandensis*), distribution of minute lateral pores on the genital double-somite (square-shaped vs. L-shaped), size of the receptaculum seminis (small vs. large), length/width ratio of the caudal rami (3 vs. 3.9), length ratio of the innermost/outermost apical setae on the caudal rami (1.2 vs. 3.1), number of setae on the basis and second endopodal segment of antenna (2 & 6 vs. 3 & 9 respectively), number of teeth on the labrum (12 vs. 10), ornamentation and shape of intercoxal sclerites in all swimming legs (with large spinules and small lateral prominences vs. smooth and with large lateral prominences), shape of the inner margin of basis and first endopodal segment of the fourth leg (convex and convex vs. straight and

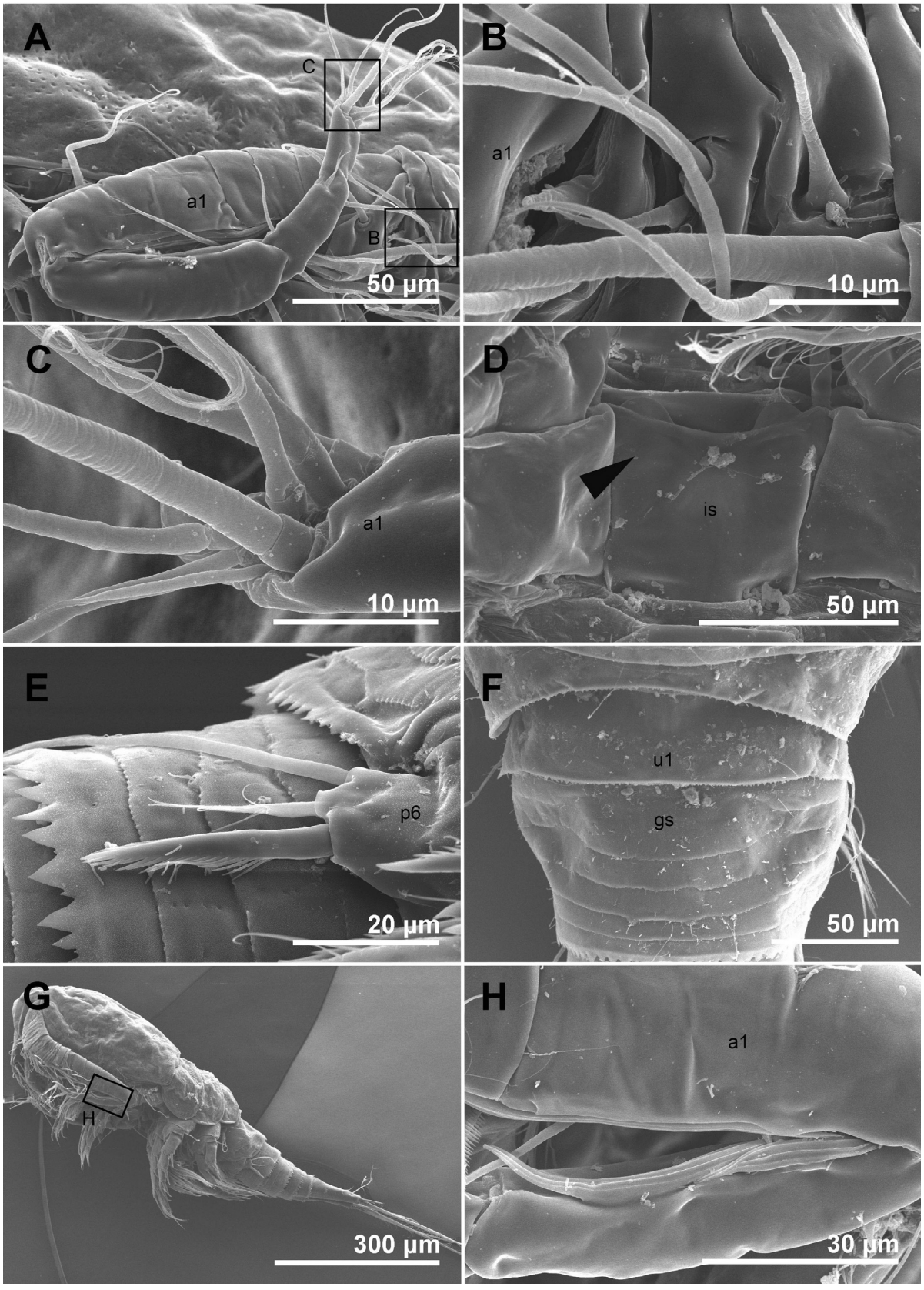

Fig. 11. *Thermocyclops thailandensis* sp. nov., SEM photographs, (A–E) paratype male 1, (F) paratype male 2, (G–H), paratype male 3: (A) antennula (a1), ventral, (B) central part of antennula (a1), ventral, (C) distal tip of antennula (a1), ventral, (D) intercoxal sclerite (is) of second swimming leg, posterior, (E) sixth leg (p6), ventral, (F) first urosomite (u1) and genital somite (gs), dorsal, (G) habitus, lateral, (H) geniculation of antennula (a1), lateral. Arrowheads indicating most prominent differences from *T. parahastatus* sp. nov. Rectangles in A and G showing areas given as close-ups in B, C, and H.

concave respectively), length ratio of the inner/outer apical spines on the fourth leg endopod (0.8 vs. 1.3), length ratio of the apical spine/seta on the fifth leg (1.3 vs. 0.7), etc. Minor distinguishing features between these two congeners include differences in surface ornamentation or proportion of armature elements on almost every segment.

Thermocyclops parahastatus, as its name suggests, is morphologically probably most similar to the African *T. hastatus* Kiefer, 1952. This species was described originally as a subspecies of *T. schmeili* (Poppe & Mrázek, 1895) from streams and ponds near Lake Kivu and Lake Edward in the Rift Valley by Kiefer (1952). Herbst (1986) elevated it to the species rank and provided additional drawings based on the holotype specimen, and Mirabdullayev et al. (2003) provided additional drawings based also on Kiefer's specimens from near Lake Edward. Morphological difference between these two congeners include: size of the receptaculum seminis (small in *T. parahastatus* vs. large in *T. hastatus*), length ratio of the inner/outer apical spines on the fourth leg endopod (0.8 vs. 0.9), length ratio of the outer apical spine/segment on the fourth leg endopod (0.9 vs 0.7), length ratio of the apical spine/seta on the fifth leg (1.3 vs. 1.7), and number of distal spinules on the intercoxal sclerite of the fourth leg (5 vs. 2 or 3). Unfortunately, the African species is still known from a limited set of morphological characters, so many appendages and most of fine ornamentation on them and on somites could not be compared. Another species that is relatively similar to *T. parahastatus* is *T. antillensis* Herbst, 1986. It was described originally as a subspecies of *T. hastatus* from a well in Guadeloupe, in the Caribbean, by Herbst (1986), but Mirabdullayev et al. (2003) elevated it to the species rank. It differs from our new species in several important morphological characters: length/width ratio of the genital double-somite (1 in *T. parahastatus* vs. 1.2 in *T. antillensis*), length ratio of the innermost/outermost apical setae on the caudal rami (1.2 vs. 0.9), length/width ratio of the ultimate antennular segment (1.8 vs. 1.5), length ratio of the inner/outer apical spines on the fourth leg endopod (0.8 vs. 0.9), length ratio of the outer apical spine/segment on the fourth leg endopod (0.9 vs 0.8), length ratio of the apical spine/seta on the fifth leg (1.3 vs. 1.7), and number and size of distal spinules on the intercoxal sclerite of the fourth leg (5 big vs. 1 or 2 small). Two other congeners that share some morphological features with *T. parahastatus* are the abovementioned African *T. schmeili* (see Kiefer 1929, 1952; Lindberg, 1951; Einsle, 1970) and the European and Central Asian *T. dybowskii* (Landé, 1890) (see Rylov, 1948; Dussart, 1969; Einsle, 1970; Monchenko, 1974; Kiefer, 1978), but all three species can be distinguished easily from each other (Mirabdullayev et al., 2003). Unfortunately no 18S or ITS data are available for any of these species yet. Therefore it was no surprise that all our molecular analyses suggested an isolated position for *T. parahastatus*. Future research should focus on molecular comparisons between morphologically very similar *T. parahastatus*, *T. hastatus*, and *T. antillensis*, as their very disjunct distribution and at least partial stygophyly might question some of our general assumptions about freshwater dispersal (Karanovic and Krajicek 2012a).

The morphology of *T. thailandensis* is such that we cannot see potential close relatives among living congeners. Some similarities are apparent with the Indian *T. marmagoensis* Sewell, 1957, which was also described originally as a subspecies of *T. schmeili* and elevated to the species rank by Mirabdullayev et al. (2003). They have a relatively similar genital double-somite, caudal rami, antenna, and swimming legs, but can be easily distinguished by their fifth legs (apical spine longer than apical seta in *T. marmagoensis* vs. shorter than apical seta in *T. thailandensis*). The 18S analysis suggested *T. thailandensis* as a sister species to an unidentified congener, albeit with a moderate support. The BI analysis of ITS suggested *T. thailandensis* as a sister clade to all *Mesocyclops* species, but this was supported very weakly and not reconstructed in the ML analysis.

In addition to the two new species, six other *Thermocyclops* are known so far from Thailand (Sanoamuang, 1998; Alekseev and Sanoamuang, 2006): *T. crassus* (Fischer, 1853); *T. decipiens* (Kiefer, 1929); *T. maheensis* (Lindberg, 1941); *T. rylovi* Smirnov, 1929; *T. taihokuensis* (Harada, 1931); and *T. wolterecki* Kiefer (1938). Additional six species have been described or reported from other countries in South East Asia (Mirabdullayev et al., 2003; Dussart and Defaye, 2006; Karanovic, 2006; Chaicharoen et al., 2011; Dela Paz et al., 2016): *T. aberrans* Lindberg (1952); *T. operculifer* (Kiefer, 1930); *T. orientalis* Dussart & Fernando (1985); *T. philippinensis* Marsh, 1932; *T. trichophorus* (Kiefer, 1930); and *T. vermifer* (Lindberg, 1935). They all differ from *T. parahastatus* and *T. thailandensis* by many morphological features, and only two of them have been sequenced for 18S and ITS (*T. crassus* and *T. decipiens*). Our molecular taxon sampling was limited by the number of available sequences on GenBank. Additional limitations included many sequences identified only to the genus level, and several sequences that could be misidentifications or contamination based on our attempts to align them unambiguously (see above). Hopefully, these results will stimulate researchers submitting sequences of unidentified specimens to at least link their data to photographs on online repositories, if not publishing results of their full morphological examination.

Surprisingly, none of our molecular analyses challenged monophyly of the genus *Mesocyclops*, despite two "feral" species in our 18S dataset, and the genus *Thermocyclops* was suggested as paraphyletic only based on the highly variable ITS region. This is encouraging because a majority of morphological characters that form diagnoses of these two genera are plesiomorphies in a larger group of cyclopoids (i.e. antennula segmentation, swimming legs segmentation and armature), and it was not clear if their major distinguishing feature (position of the large spine on the fifth leg) is an apomorphy or not (Lindberg, 1942; Rylov, 1948; Einsle, 1970; Ueda and Reid, 2003; Hołyńska, 2006). The fact that we analysed them together with the supposedly closely related genera *Cyclops* and *Diacyclops*, which also differ mostly in the position of the spine (albeit considerably smaller one) on the fifth leg, adds more weight to this morphological character (or a set of characters). In reality, the only difference between *Cyclops* and *Mesocyclops*, as well as between *Diacyclops* and *Thermocyclops*, is the relative length of this armature element, and it would be easy to imagine it convergently getting reduced in size (or enlarged) numerous times (Huys and Boxshall, 1991; Monchenko and Von Vaupel Kelin, 1999). However, this seems to be not the norm, at least not in our very limited dataset. Leaving aside potential misidentifications and contaminations for both genes and in both genera, which could not be unquestionably aligned with the rest of taxa (see above), three "feral" species in the 18S dataset deserve further mention: *M. dissimilis* Defaye and Kawabata, 1993; *M. darwini* Dussart and Fernando, 1988; and *D. uruguayensis* (Kiefer, 1935). As mentioned in the Results, *M. dissimilis* and *D. uruguayensis* did introduce one gap in our alignment (their sequences being one base longer than the rest), but apart from that their sequences were aligned extremely well with all others, with numerous very conservative blocks. All three species also differed mostly from other species in the area around this gap, so there is a possibility that the original editing and/or weak sequencing signal might have some influence on their unusual phylogenetic position. There is nothing in the external morphology of either the Japanese *M. dissimilis* or the Australian *M. darwini* to suggest them as distant from the rest of their congeners, and certainly nothing that would suggest *M. darwini* as a member of the genus *Thermocyclops* (see Dussart and Fernando, 1988; Defaye and Kawabata, 1993; Mirabdullayev et al., 2003). Also, in the ITS cladogram, *M. darwini* clustered together with the rest of its congeners (ITS sequences of *M. dissimilis* are as yet unavailable).

Wyngaard et al. (2010) also noted that the position of *M. darwini* in the genus did vary depending on the characters used, so it is possible that its 18S sequence is indeed problematic. The 18S sequence of *D. uruguayensis* was already considered problematic by Karanovic and Krajicek (2012b), who excluded it from their analysis of the genus *Diacyclops*. However, morphologically this species does stand out from a majority of *Diacyclops* species, and seems to form a distinct group with several other American congeners (Kiefer, 1935; Reid, 1998; Fiers et al., 2000). It is possible that this group could be one of those convergent evolutionary events that could challenge monophyly of some well-established cyclopoid genera based mostly on the fifth leg shape. Karanovic and Krajicek (2012b) also excluded from their analysis several unpublished and unidentified short fragments of 18S *Diacyclops* sequences from Lake Baikal that are available from GenBank, considering them either a contamination or misidentification. However, several near complete 18S sequences in our analysis allowed us to align these fragments unambiguously, but they were not overlapping with other fragments and were therefore excluded. Congruence between our 18S tree and that of Karanovic and Krajicek (2012b) based on 12S, suggesting the Australian *D. scanloni* as a sister clade to all other *Diacyclops*, inspires confidence in phylogenetic reconstructions of cyclopoids based on molecular data.

Phylogenetic reconstructions based on morphological data are extremely rare in freshwater cyclopoids, notable exceptions being those by Hołyńska (2006) for the genus *Mesocyclops* (also repeated in Wyngaard et al., 2010) and Karanovic et al. (2011) of small Australian cyclopoids. We consider the former slightly problematic, because out of 81 characters 40 contained at least one ambiguous character state, 12 contained two or more ambiguous character states, and 17 were this exact character state structure: (0) present; (1) present or absent; (2) absent. A much more productive approach in cladistic analysis is when individual armature elements (setae and spines) or ornamentation (such as spinules and cuticular organs) are homologized (Karanovic, 2010, 2014; Karanovic et al., 2013; Karanovic and Kim, 2014) than when their total number is scored as a character state (for example, characters 27 and 80 in Hołyńska, 2006 and Wyngaard et al., 2010). Recent developments in copepod species delimitation and description through congruence between molecular data and quantitative shape analysis explicitly challenge the concept of cryptic and/or polymorphic species (Karanovic et al., 2016), and many currently valid and widely distributed *Mesocyclops* and *Thermocyclops* species, with apparently wide intraspecific variation in morphological characters, will probably be exposed as species complexes (Bláha et al., 2010; Hamrova et al., 2012; Karanovic and Krajicek, 2012a).

Acknowledgements

This work was supported by a grant from the National Institute of Biological Resources (NIBR), funded by the ministry of Environment (MOE) of the Republic of Korea (NIBR201704101), to the first author. The scanning electron microscope was made available through the courtesy of Prof. Jin Hyun Jun (Eulji University, Seoul), and we also want to thank Mr. Junho Kim (Eulji University, Seoul) for the technical help provided. The first author is grateful to the Applied Taxonomic Research Center of Khon Kaen University for financial support of his visit to Thailand. Remarks from two anonymous reviewers improved the manuscript considerably, and we also thank Dr. Joachim T. Haug (Ludwig-Maximilians-Universität, München) for his careful edits.

Appendix A. Supplementary data

Supplementary data associated with this article can be found, in the online version, at http://dx.doi.org/10.1016/j.jcz.2017.07.003.

References

Alekseev, V.R., Sanoamuang, L., 2006. Biodiversity of cyclopoid copepods in Thailand –with a description of *Afrocyclops henrii* spn. Arthropoda Selecta 15, 277–290.
Altschul, S.F., Gish, W., Miller, W., Myers, E.W., Lipman, D.J., 1990. Basic local alignment search tool. J. Mol. Biol. 215, 403–410.
Bláha, M., Hulák, M., Slouková, J., Těšitel, J., 2010. Molecular and morphological patterns across *Acanthocyclops vernalis-robustus* species complex (Copepoda, Cyclopoida). Zoologica Scripta 39, 259–268.
Burton, R.S., Lee, B.N., 1994. Nuclear and mitochondrial gene genealogies and allozyme polymorphism across a major phylogeographic break in the copepod *Tigriopus californicus*. Proc. Natl. Acad. Sci. U. S. A. 91, 5197–5201.
Carstens, B.C., Pelletier, T.A., Reid, N.M., Satler, J.D., 2013. How to fail at species delimitation. Mol. Ecol. 22, 4369–4383.
Chaicharoen, R., Sanoamuang, L., Hołyńska, M., 2011. A review of the genus *Thermocyclops* (Crustacea: copepoda: Cyclopoida) in Cambodia. Zool. Stud. 50, 780–803.
Darriba, D., Taboada, G.L., Doallo, R., Posada, D., 2012. jModelTest 2: more models, new heuristics and parallel computing. Nat. Methods 9, 772.
Defaye, D., Kawabata, K., 1993. *Mesocyclops dissimilis* n. sp. from lake biwa Japan (Copepoda, Cyclopoida). Hydrobiologia 257, 121–126.
Dela Paz, E.S.P., Hołyńska, M.K., Papa, R.D.S., 2016. *Mesocyclops* and *Thermocyclops* (Copepoda, Cyclopidae) in the major visayas islands (Central Philippines). Crustaceana 89, 787–809.
Denis, F., Ravallec, R., Pavillon, J.F., Wormhoudt, A.V., 2009. Genetic differentiation of Atlantic populations of the intertidal copepod Tigriopus brevicornis. Sci. Mar. 73, 579–587.
Duchovnay, A., Reid, J.W., McIntosh, A., 1992. Thermocyclops crassus (Crustacea: Copepoda) present in nort america: a new record from lake champlain. J. Great Lakes Res. 18, 415–419.
Dumont, H.J., Maas, S., 1985. *Mesocyclops cuttacuttae* n. sp. from a cave in northern Australia (Crustacea: Copepoda, Cyclopoida). Beagle 1, 115–122.
Dussart, B., Defaye, D., 2006. World Directory of Crustacea Copepoda of Inland Waters, II – Cyclopiformes. Backhuys Publishers, Leiden, The Netherlands, 354 pp.
Dussart, B.H., Fernando, C.H., 1988. Sur quelques mesocyclops (Crustacea, Copepoda). Hydrobiologia 157, 241–264.
Dussart, B.H., 1969. Cyclopoïdes et Biologie, Les Copépodes des eaux continentales d'Europe occidentale, vol. 2. Boubee & Cie, Paris, pp. 292.
Edmands, S., 2001. Phylogeography of the intertidal copepod Tigriopus californicus reveals substantially reduced population differentiation at northern latitudes. Mol. Ecol. 10, 1743–1750.
Einsle, U. (1970). Études morphologiques sur des espéces de Thermocyclops (Crust. Cop.) d'Afrique et d'Europe. Cahiers Office de la recherche Scientifique et Technique Outre-Mer, Series Hydrobiology (ORSTOM) 4, 13–38.
Ellison, C.K., Burton, R.S., 2008. Interpopulation hybrid breakdown maps to the mitochondrial genome. Evolution 62, 631–638.
Felsenstein, J., 1985. Confidence limits on phylogenies: an approach using the bootstrap. Evolution 39, 783–791.
Fiers, F., Reid, J.W., Iliffe, T.M., Suárez-Morales, E., 1996. New hypogean cyclopoid copepods (Crustacea) from the Yucatán peninsula. Contrib. Zool. 66, 65–102.
Fiers, F., Ghenne, V., Suárez-Morales, E., 2000. New species of continental cyclopoid copepods (Crustacea Cyclopoida) from the Yucatán peninsulaMexico. Stud. Neotropic. Fauna Environ. 35, 209–251.
Ganz, H.H., Burton, R.S., 1995. Genetic differentiation and reproductive incompatibility among Baja California populations of the copepod *Tigriopus californicus*. Mar. Biol. 123, 821–827.
Goetze, E., 2003. Cryptic speciation on the high seas; global phylogenetics of the copepod family Eucalanidae. Proc. R. Soc. Lond. Ser. B 270, 2321–2331.
Gophen, M., 1986. Mesocyclops and thermocyclops populations in lake kinneret (Israel). Syllogeus 58, 294–299.
Guindon, S., Gascuel, O., 2003. A simple: fast and accurate method to estimate large phylogenies by maximum-likelihood. Syst. Biol. 52, 696–704.
Gutiérrez-Aguirre, M., Suárez-Morales, E., 2000. The eurasian *Thermocyclops crassus* (Fischer 1853) (Copepoda, Cyclopoida) found in southeastern Mexico. Crustaceana 73, 705–713.
Hamrova, E., Krajicek, M., Karanovic, T., Cerny, M., Petrusek, A., 2012. Congruent patterns of lineage diversity in two species complexes of planktonic crustaceans, *Daphnia longispina* (Cladocera) and Eucyclops serrulatus (Copepoda), in East European mountain lakes. Zool. J. Linnaean Soc. 166, 754–767.
Handschumacher, L., Steinarsdóttir, M.B., Edmands, S., Ingólfsson, A., 2010. Phylogeography of the rock-pool copepod *Tigriopus brevicornis* (Harpacticoida) in the northern North Atlantic, and its relationship to other species of the genus. Mar. Biol. 157, 1357–1366.
Herbst, H.-V., 1986. Beschreibung des *Thermocyclops hastatus antillensis* n. ssp. mit einem Bestimmungsschlüssel für die Gattung Thermocyclops Kiefer, 1927. Bijdragen tot de Dierkunde 56, 165–180.
Hołyńska, M., Reid, J.W., Ueda, H. (2003) Genus Mesocyclops Sars, 1914. In: Ueda, H. & J.W. Reid (Eds), Copepoda: Cyclopoida, Genera Mesocyclops and Thermocyclops, Guides to the Identification of the Microinvertebrates of the Continental Waters of the World. H.J.F. Dumont (Ed.). Backhuys Publishers, Leiden, The Netherlands,V olume 20, pp. 12–213.

Hołyńska, M., 1994. A redescrption of *Mesocyclops thermocyclopoides* harada 1931 (Copepoda, Cyclopidae). Bulletin de l'Institut Royal des Sciences Naturelles de Belgique Biologie 64, 99–110.
Hołyńska, M., 2006. Phylogeny of *Mesocyclops* (Copepoda: Cyclopidae) interred from morphological characters. Zool. J. Linn. Soc. 147, 1–70.
Huelsenbeck, J.P., Ronquist, F., 2001. MRBAYES: Bayesian inference of phylogeny. Bioinformatics 17, 754–755.
Hurvich, C.M., Tsai, C.L., 1989. Regression and time series model selection in small samples. Biometrika 76, 297–307.
Huys, R., Boxshall, G.A., 1991. Copepod Evolution. The Ray Society, London, UK, p.468.
Huys, R., Llewellyn-Hughes, J., Olson, P.D., Nagasawa, K., 2006. Small subunit rDNA and Bayesian inference reveal *Pectenophilus ornatus* (Copepoda *incertae sedis*) as highly transformed Mytilicolidae, and support assignment of Chondracanthidae and Xarifiidae to Lichomolgoidea (Cyclopoida). Biol. J. Linnaean Soc. 87, 403–425.
Huys, R., Fatih, F., Ohtsuka, S., Llewellyn-Hughes, J., 2012. Evolution of the bomolochiform superfamily complex (Copepoda: Cyclopoida): New insights from ssrDNA and morphology, and origin of umazuracolids from polychaete-infesting ancestors rejected. Int. J. Parasitol. 42, 71–92.
Hwang, A.S., Northrup, S.L., Peterson, D.L., Kim, Y., Edmands, S., 2012. Long-term experimental hybrid swarms between nearly incompatible *Tigriopus californicus* populations: persistent fitness problems and assimilation by the superior population. Conserv. Genet. 13, 567–579.
Ito, T., 1970. Groundwater copepdos from the western part of Japan. Japn. J. Limnol. 21, 131–140.
Karanovic, T., Cooper, S.J.B., 2011a. Molecular and morphological evidence for short-range endemism in the *Kinnecaris solitaria* complex (Copepoda: Parastenocarididae), with descriptions of seven new species. Zootaxa 3026, 1–64.
Karanovic, T., Cooper, S.J.B., 2011b. Third genus of paratenocaridid copepods from Australia supported by molecular evidence (Copepoda, Harpacticoida). In: Defaye, D., Suárez-Morales, E., von Vaupel Klein, J.C. (Eds.), 'Crustaceana Monographs, Studies on Freshwater Copepoda: a Volume in Honour of Bernard Dussart'. Brill, Leiden, Netherlands, pp. 293–337.
Karanovic, T., Cooper, S.J.B., 2012. Explosive radiation of the genus *Schizopera* on a small subterranean island in Western Australia (Copepoda: Harpacticoida): unravelling the cases of cryptic speciation, size differentiation and multiple invasions. Invertebrate Syst. 26, 115–192.
Karanovic, T., Kim, K., 2014. Suitability of cuticular pores and sensilla for harpacticoid copepod species delineation and phylogenetic reconstruction. Arthropod Struct. Dev. 43, 615–658.
Karanovic, T., Krajicek, M., 2012a. When anthropogenic translocation meets cryptic speciation globalised bouillon originates; molecular variability of the cosmopolitan freshwater cyclopoid *Macrocyclops albidus* (Crustacea: Copepoda). Int. J. Limnol. 48, 63–80.
Karanovic, T., Krajicek, M., 2012b. First molecular data on the Western Australian *Diacyclops* (Copepoda: Cyclopoida) confirm morphospecies but question size differentiation and monophyly of the *alticola*-group. Crustaceana 85, 1549–1569.
Karanovic, T., Eberhard, S.M., Murdoch, A., 2011. A cladistic analysis and taxonomic revision of Australian *Metacyclops* and *Goniocyclops*, with description of four new species and three new genera (Copepoda, Cyclopoida). Crustaceana 84, 1–67.
Karanovic, T., Eberhard, S.M., Perina, G., Callan, S., 2013. Two new subterranean ameirids (Crustacea: Copepoda: Harpacticoida) expose weaknesses in the conservation of short-range endemics threatened by mining developments in Western Australia. Invertebrate Syst. 27, 540–566.
Karanovic, T., Djurakic, M., Eberhard, S., 2016. Cryptic species or inadequate Taxonomy?: Implementation of 2D geometric morphometrics based on integumental organs as landmarks for delimitation and description of copepod taxa. Syst. Biol. 65, 304–327.
Karanovic, T., 2000. On *Reidcyclops*, new genus (Crustacea, Copepoda), with the first description of the male of *Reidcyclops trajani* (Reid & Strayer, 1994), new combination. Beaufortia 50, 79–88.
Karanovic, T., 2006. Subterranean copepods (Crustacea, Copepoda) from the pilbara region in western Australia. Rec. Western Aust. Mus., 1–239.
Karanovic, T., 2010. First record of the harpacticoid genus *Nitocrellopsis* (Copepoda Ameiridae) in Australia, with descriptions of three new species. Int. J. Limnol. 46, 249–280.
Karanovic, T., 2014. On the phylogeny of Euryteinae (Crustacea Copepoda, Cyclopoida), with description of one new species from Korea. Zool. Anz. 253, 512–525.
Ki, J.-S., Lee, K.-W., Park, H.G., Chullasorn, S., Dahms, H.-U., Lee, J.-S., 2009. Phylogeography of the copepod *Tigriopus japonicus* along the Northwest Pacific rim. J. Plankton Res. 31, 209–221.
Kiefer, F., 1927. Beiträge zur Copepodenkunde (VI). Zool. Anz. 74, 116–122.
Kiefer, F., 1929. Crustacea Copepoda, 2. Cyclopoida Gnathostoma. Das Tierreich, Berlin and Leipzig (100 pp).
Kiefer, F., 1935. Neue Süsswassercyclopiden (Crustacea Copepoda) aus Uruguay. Zool. Anz. 109, 181–188.
Kiefer, F., 1952. Copepoda Calanoida und Cyclopoida. *Exploration du Parc National Albert Mission H. Damas (1935–1936)*. Institut des Parcs Nationaux du Congo Belge 21, 1–136.
Kiefer, F., 1978. Freilebende Copepoda. In: Kiefer, F., Fryer, G. (Eds.), Das Zooplankton Der Binnengewässer. Binnengewässer, 2. Teil, 26(2): pp. 1–380.
Kimura, M., 1980. A simple method for estimating evolutionary rates of base substitutions through comparative studies of nucleotide sequences. J. Mol. Evol. 16, 111–120.
Kumar, S., Stecher, G., Tamura, T., 2016. MEGA 7: molecular evolutionary genetics analysis version 7.0 for bigger datasets. Mol. Biol. Evol. 33, 1870–1874.
Lee, C.E., Remfert, J.L., Gelembiuk, G.W., 2003. Evolution of physiological tolerance and performance during freshwater invasions. Integr. Comp. Biol. 43, 439–449.
Lindberg, K., 1942. Cyclopides (Crustacés Copépodes) de l'Inde, XIV–XVIII. Rec. Indian Mus. 44, 139–190.
Lindberg, K., 1951. Cyclopides de Madagascar. Mémoires de l'Institut Scientifique de Madagascar (A) 6, 427–437.
Maier, G., 1996. Copepod communities in lakes of varying trophic degree. Archiv für Hydrobiologie 136, 455–465.
Marshall, J.C., Arevalo, E., Benavides, E., Sites, J., Sites Jr., J.W., 2006. Delimiting species: comparing methods for Mendelian characters using lizards of the *Sceloporus grammicus* (Squamata: Phrynosomatidae) complex. Evolution 60, 1050–1065.
Mirabdullayev, I.M., Reid, J.W., Ueda, H. (2003) Genus Mesocyclops Sars, 1914. In: Ueda, H. & J.W. Reid (Eds), Copepoda: Cyclopoida, Genera Mesocyclops and Thermocyclops, Guides to the Identification of the Microinvertebrates of the Continental Waters of the World. H.J.F. Dumont (Ed.). Backhuys Publishers, Leiden, The Netherlands, Vol. 20, pp. 214–302.
Monchenko, V.I., Von Vaupel Kelin, J.C., 1999. Oligomerization in Copepoda Cyclopoida as a kind of orthogenetic evolution in the animal kingdom. Crustaceana 72, 241–264.
Monchenko, V.I., 1974. Shchelepnoroti Tsiklopodiny, Tsiklopi (Cyclopidae), vol. 27. Fauna Ukrainy, Vidavnitstvo Naukova Dumka, Kiev (3) 452 pp [in Ukrainian].
Padial, J.M., Miralles, A., De la Riva, I., Vences, M., 2010. The integrative future of taxonomy. Front. Zool. 7, 16.
Palmer, C.A., Edmands, S., 2000. Mate choice in the face of both inbreeding and outbreeding depression in the intertidal copepod *Tigriopus californicus*. Mar. Biol. Berl. 136, 693–698.
Pesce, G.L., Maggi, D., 1981. Cyclopides et Calanoides des eaux phréatiques de la Grèce meridionale et insulaire (Crustacea: Copepoda). Ecologia Méditerranea 7, 164–812.
Peterson, D.L., Kubow, K.B., Connolly, M.J., Kaplan, L.R., Wetkowski, M.M., Leong, W., Phillips, B.C., Edmands, S., 2013. Reproductive and phylogenetic divergence of tidepool copepod populations across a narrow geographical boundary in Baja California. J. Biogeogr. 40, 1664–1675.
Pons, J., Barraclough, T.G., Gmoez-Zurita, J., Cardoso, A., Duran, D.P., Hazell, S., Kamoun, S., Sumlin, W.D., Vogler, A.P., 2006. Sequence-based species delimitation for the DNA taxonomy of undescribed insects. Syst. Biol. 55, 595–609.
Reid, J.W., 1993. New records and redescriptions of American species of *Mesocyclops* and of *Diacyclops bernardi* (Petkovski, 1986) (Copepoda: Cyclopoida). Bijdragen tot de Dierkunde 63, 173–191.
Reid, J.W., 1998. Redescription and first records from Brazil of *Diacyclops uruguayensis* kiefer (Crustacea, Copepoda, Cyclopidae). Revista Brasileira de Zoologia Curitiba 15, 757–766.
Reid, J.W. (2003) Evolution and Biology. In: Ueda, H. & J.W. Reid (Eds), Copepoda: Cyclopoida, Genera Mesocyclops and Thermocyclops, Guides to the Identification of the Microinvertebrates of the Continental Waters of the World. H.J.F. Dumont (Ed.). Backhuys Publishers, Leiden, The Netherlands, Volume 20, pp. 5–8.
Rodríguez, F., Oliver, J.F., Marín, A., Medina, J.R., 1990. The general stochastic model of nucleotide substitutions. J. Theor. Biol. 142, 485–501.
Ronquist, F., Huelsenbeck, J.P., 2003. MRBAYES 3: Bayesian phylogenetic inference under mixed models. Bioinformatics 19, 1572–1574.
Ronquist, F., Tesleno, M., van den Mark, P., Ayes, D.L., Darling, A., Höhna, S., Larget, B., Liu, L., Suchard, M.C., Huelsenbeck, J.P., 2012. Mr Bayes 3.2: Efficient Bayesian phylogenetic inference and model Choice across a large model space. Syst. Biol. 62, 539–542.
Ruttner, F., 1952. Planktonstudien der Deutschen Limnologischen Sunda-Expedition. Archiv für Hydrobiologie (Supplementband 21), 1–271.
Rylov, V.M., 1948. Crustacea, Freshwater Cyclopoida. Fauna of the U.S.S.R. (in Russian).
Sanoamuang, L., 1999. Species composition and distribution of freshwater Calanoida and Cyclopoida (Copepoda) of northeast Thailand. Amsterdam, The Netherlands, July 20–24, 1998. In: Schram, F.R., von Vaupel Klein, J.C. (Eds.), Crustaceans and the Biodiversity Crisis. Proceedings of the Fourth International Crustacean Congress, vol. I. Koninklijke Brill, Leiden, pp. 217–230.
Spears, T., Abele, L.G., Kim, W., 1992. The monophyly of brachyuran crabs: a phylogenetic study based on 18S rRNA. Syst. Biol. 41, 446–461.
Stock, J.K., von Vaupel Klein, J.C., 1996. Mounting media revisited: the suitability of Reyne's fluid for small crustaceans. Crustaceana 69, 794–798.
Thompson, J.D., Higgins, D.G., Gibson, T.J., 1994. CLUSTAL W: improving the sensitivity of progressive multiple sequence alignment through sequence weighting, position-specific gap penalties and weight matrix choice. Nucleic Acids Res. 22, 4673–4680.
Ueda, H., Reid, J.W. (2003) Introduction. In: Ueda, H. & J.W. Reid (Eds), Copepoda: Cyclopoida, Genera Mesocyclops and Thermocyclops, Guides to the Identification of the Microinvertebrates of the Continental Waters of the World. H.J.F. Dumont (Ed.). Backhuys Publishers, Leiden, The Netherlands,V olume 20, pp. 3–5.

Van de Velde, I., 1987. New *Mesocyclops* species (Copepoda Cyclopidae) from Papua New Guinea. Bulletin de l'Institut Royal des Sciences Naturelles de Belgique Biologie 57, 149–162.
Vogt, N.B., 2013. Temple Caves and Grottoes in Thailand, a Picture-guide Book. Booksmango, Thailand, pp. 166.
White, T.J., Bruns, T., Lee, S., Taylor, J., 1990. Amplification and direct sequencing of fungal ribosomal RNA genes for phylogenetics. In: Innis, M.A., Gelfand, D.G., Sninsky, J.J., White, T.J. (Eds.), PCR Protocols: A Guide To Methods and Applications. Academic Press, London, pp. 315–322.
Wiens, J.J., 2007. Species delimitation: new approaches for discovering diversity. Syst. Biol. 56, 875–878.
Will, K.W., Mishler, B.D., Wheeler, Q.D., 2005. The perils of DNA barcoding and the need for integrative taxonomy. Syst. Biol. 54, 844–851.
Williamson, C.E., 1986. The swimming and feeding of *Mesocyclops*. Hydrobiologia 134, 11–19.
Winkler, G., Dodson, J.J., Lee, C.E., 2008. Heterogeneity within the native range: population genetic analyses of sympatric invasive and noninvasive clades of the freshwater invading copepod *Eurytemora affinis*. Mol. Ecol. 17, 415–430.
Wyngaard, G.A., Hołyńska, M., Schulte II, J.A., 2010. Phylogeny of the freshwater copepod *Mesocyclops* (Crustacea: Cyclopidae) based on combined molecular and morpholoical data, wih notes on biogeography. Mol. Phylogenet. Evol. 55, 753–764.